Friedrich-Alexander-Universität
Erlangen-Nürnberg

Erlangen Centre for Astroparticle Physics

Cosmic Ray escape from Galactic PeVatrons

CDHY PeVatron Workshop

Alison Mitchell
Junior Research Group Leader
10th October 2025

Emmy Noether-Programm
Funded by DFG Deutsche Forschungsgemeinschaft German Research Foundation

Galactic PeVatrons & UHE sources

PeVatron = accelerator to PeV
—> capability of reaching $\gtrsim 10^{15}$ eV particle energy

To detect a PeVatron, need to convolve this with:

—> duration over which acceleration to $\gtrsim 10^{15}$eV occurs
—> fraction of CRs that escape vs remain in vicinity of accelerator

For UHE sources ($E_\gamma \geq 100\,\mathrm{TeV}$) one needs:

—> sufficient number of energetic particles in a location
—> sufficient target (matter, radiation) for particle interactions

$N_{\mathrm{UHE}} \neq N_{\mathrm{PeVatron}}$ i.e. not necessarily a one-to-one correspondence

This talk: a brief look at some examples of CR escape from SNRs, Stellar clusters and PWNe / halos.

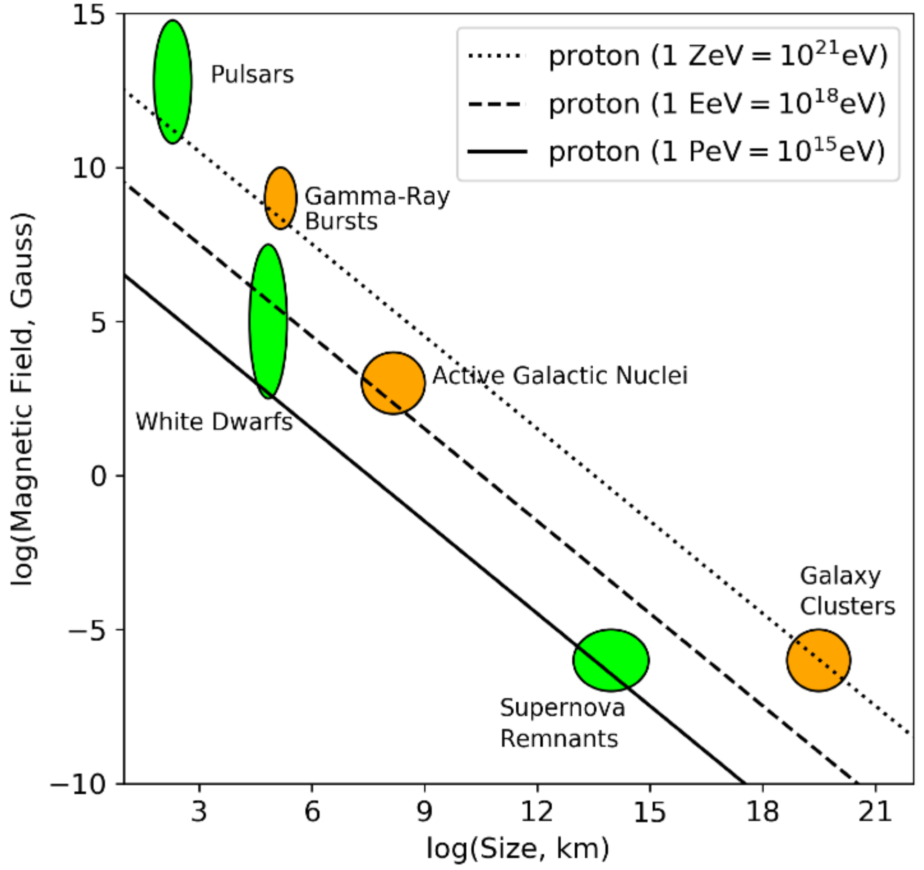

Hillas condition: $E_{\mathrm{max}} = Ze\beta cBL$

Supernova Remnants

- Prime PeVatron candidates —> yet spectrum ends ~100 TeV and recent estimates of SN rate ~0.4-0.5 per century Quintana et al. (2025)
- Only act as PeVatrons for a short time?
- Escaping cosmic rays may illuminate nearby clouds —> detailed knowledge of clouds required!

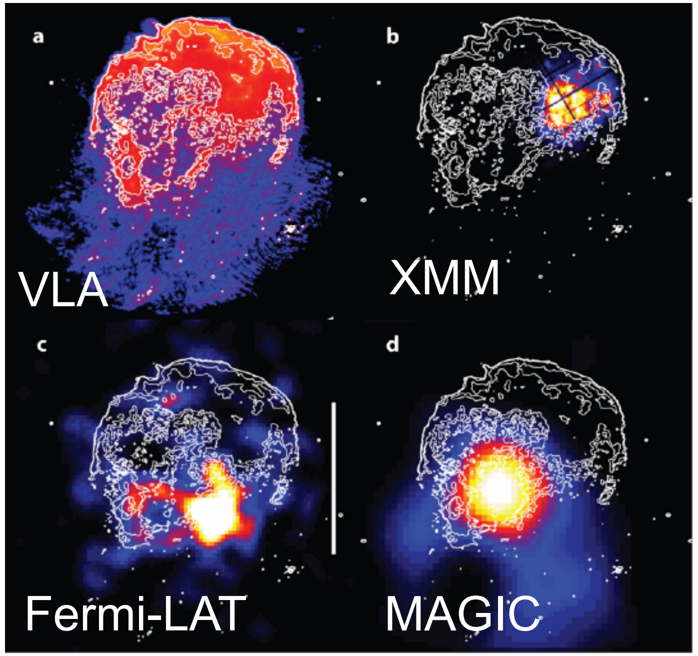

Funk S. 2015. Annu. Rev. Nucl. Part. Sci. 65:245–77

IC 443

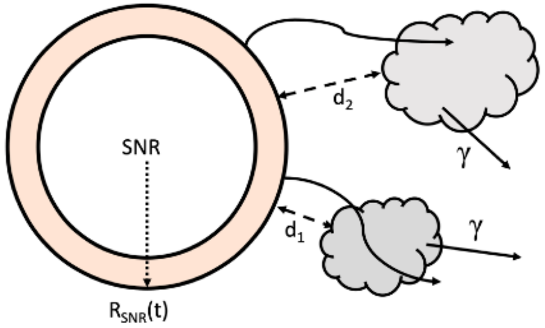

AM et al. 2021

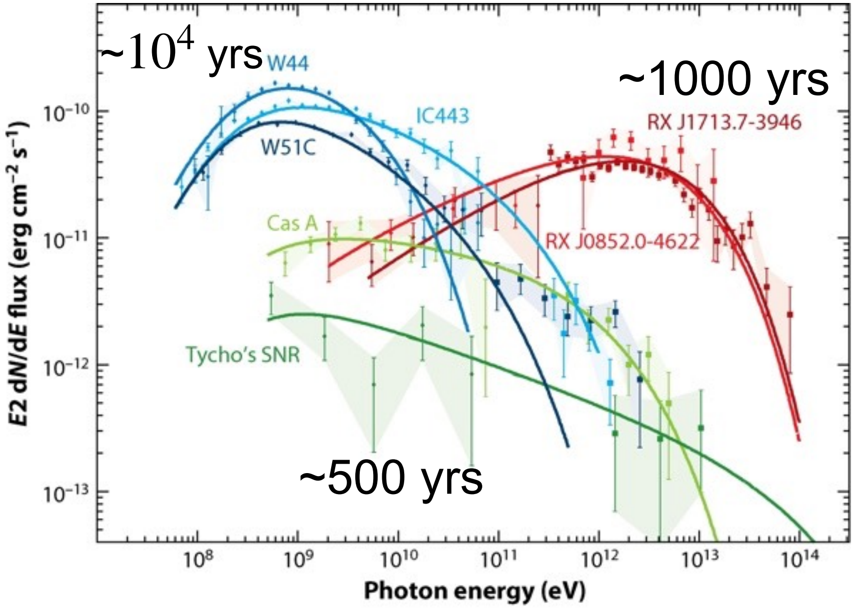

Funk S. 2015. Annu. Rev. Nucl. Part. Sci. 65:245–77

CR escape from Supernova Remnants

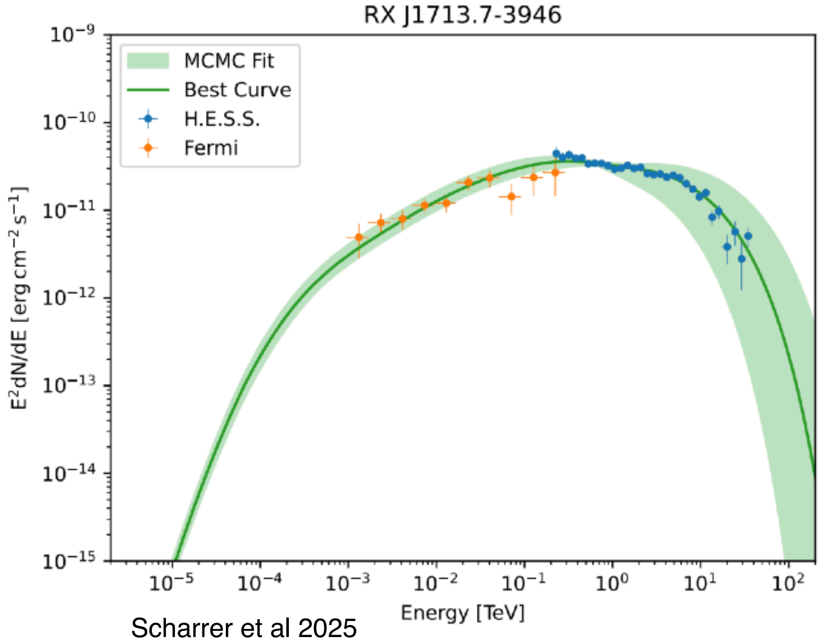

Scharrer et al 2025

Assume SNRs reach their maximum energy (1 PeV) at the Sedov time

After which particles escape in an energy-dependent manner:

$$t_{\rm esc} = t_{\rm sed} \left(\frac{p}{p_M} \right)^{-1/\beta} \text{yr.}$$

..and then diffuse through the ISM.

Spectrum of particles arriving at a cloud can be much harder than that at the accelerator

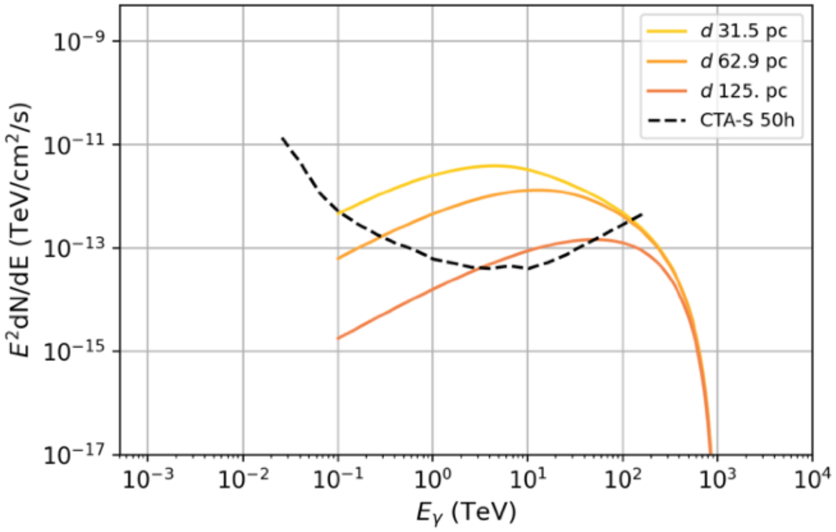

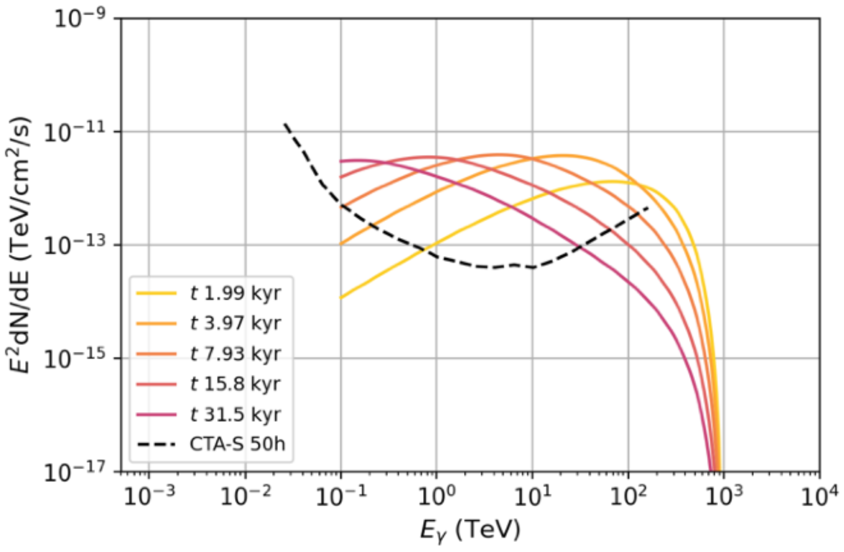

AM et al. 2021

Example: LHAASO J2108+5157

Apply model to LHAASO J2108+5157

Unidentified LHAASO source (dark) yet coincident with two clouds.

Adopt for the two clouds "MML[2017]4607" (solid) and "FKT[2022]" (dashed) the models that best match the data

Vary properties of the cloud according to the quoted uncertainties in measured parameters (or ~10% minimum uncertainty assumed)

Cloud	MML[2017]4607	FKT[2022]
(l (deg), b (deg))	(92.272, 2.775)	(92.4, 3.2)
d (kpc)	3.28	1.7 ± 0.6
n (cm^{-3})	30	37 ± 14
Size (deg)	0.5	1.1 ± 0.2

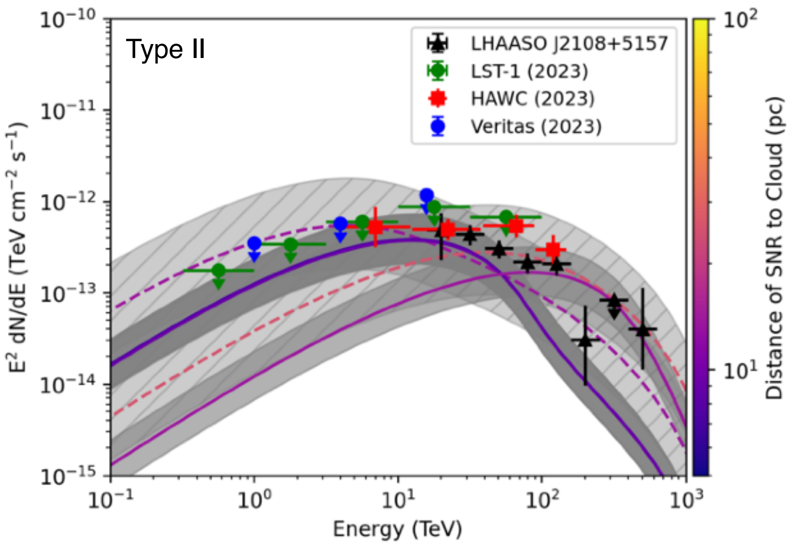

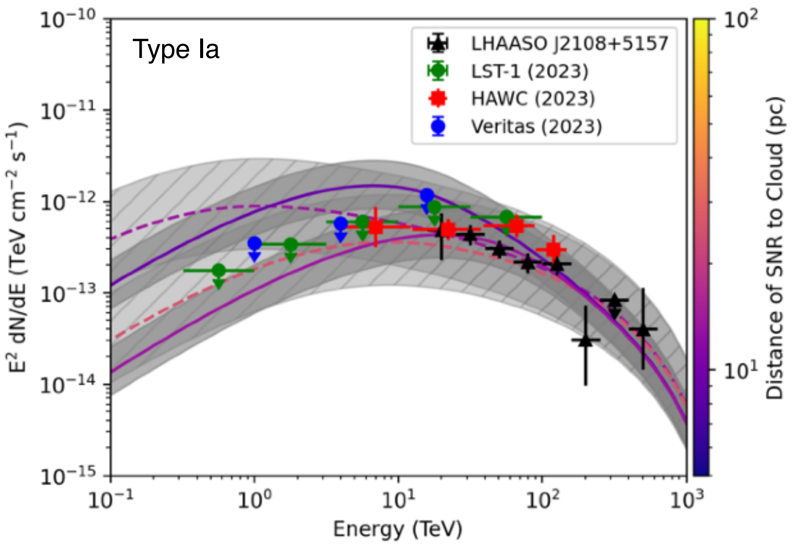

Cloud	t (kyr)	Δd (pc)	SN type	χ^2
MML[2017]4607	1	37	Ia	5.1
FKT[2022]	4	37 *	Ia	6.7
FKT[2022]	4	57	Ia	9.3
FKT[2022]	4	57	II	15.5
FKT[2022]	8	24 **	II	17.0
MML[2017]4607	4	24 **	II	24.4
MML[2017]4607	2	37	II	25.0
MML[2017]4607	1	24	Ia	28.2

AM 2024

SNR illuminated clouds explaining unidentified sources?

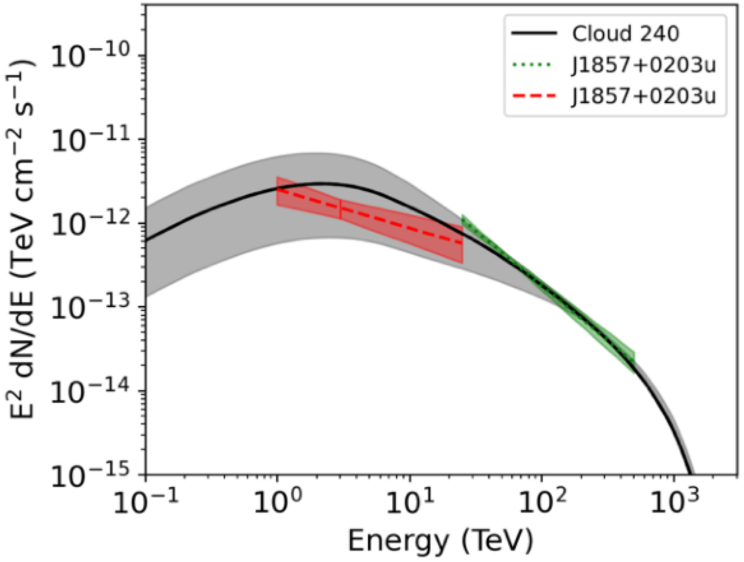

Can search systematically:

— identify clouds potentially illuminated by nearby SNRs
— identify coincidence with LHAASO unidentified sources
— compare spectra to identify potential contributions

—> heavily reliant on completeness of catalogues used

Rice et al 2016, Cao et al. 2024, Ferrand & Safi-Harb 2012

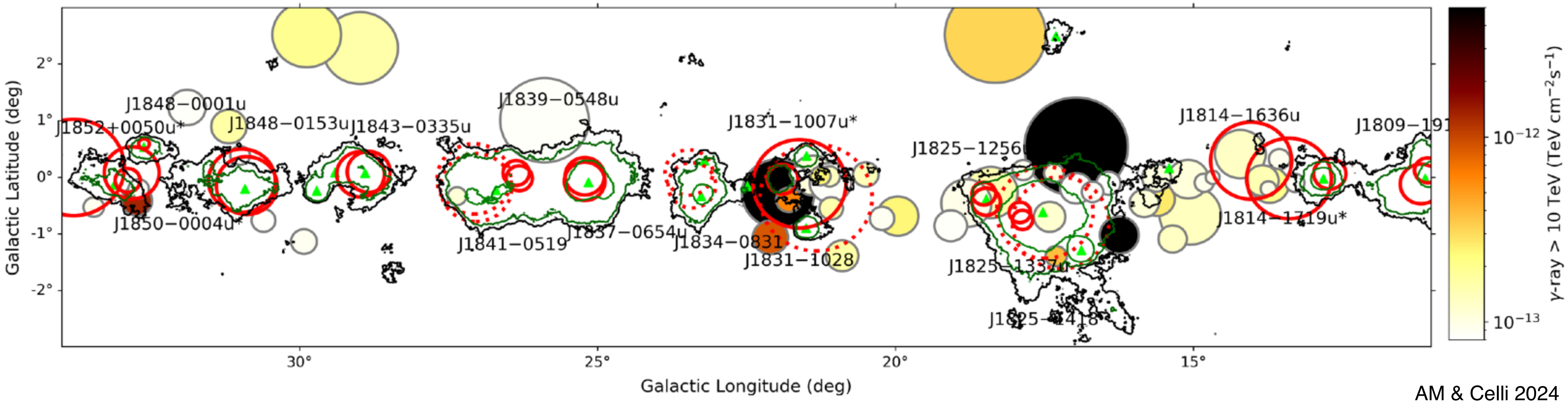

AM & Celli 2024

Observed examples: interacting SNRs and nearby clouds

RX J1713.7-3946
Evidence for gamma-rays extending beyond the X-ray shell and shock interaction with molecular material (CO, HI) surrounding the SNR

HESS J1731-347 & HESS J1729-345
SNR illuminating nearby molecular clouds?

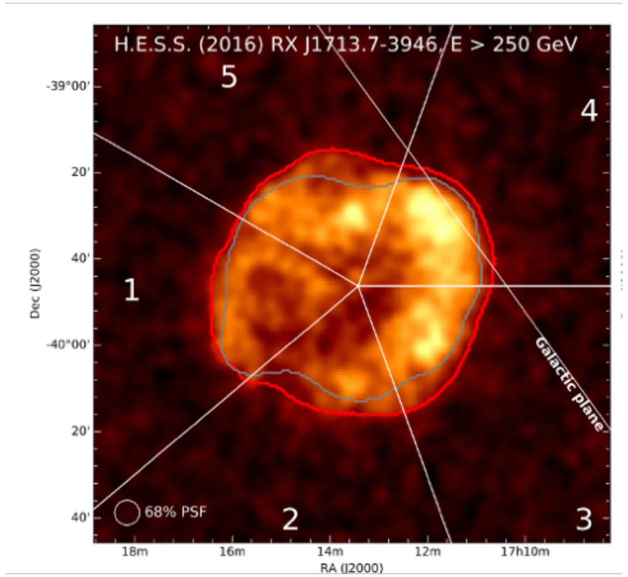

HESS coll. 2018

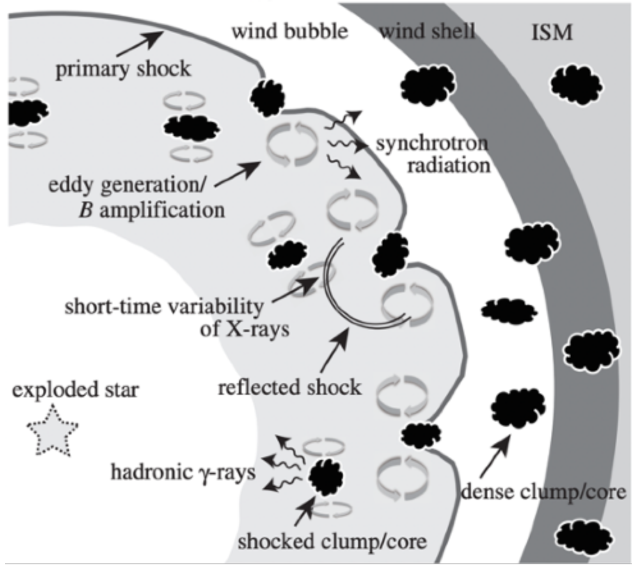

Inoue et al. 2012

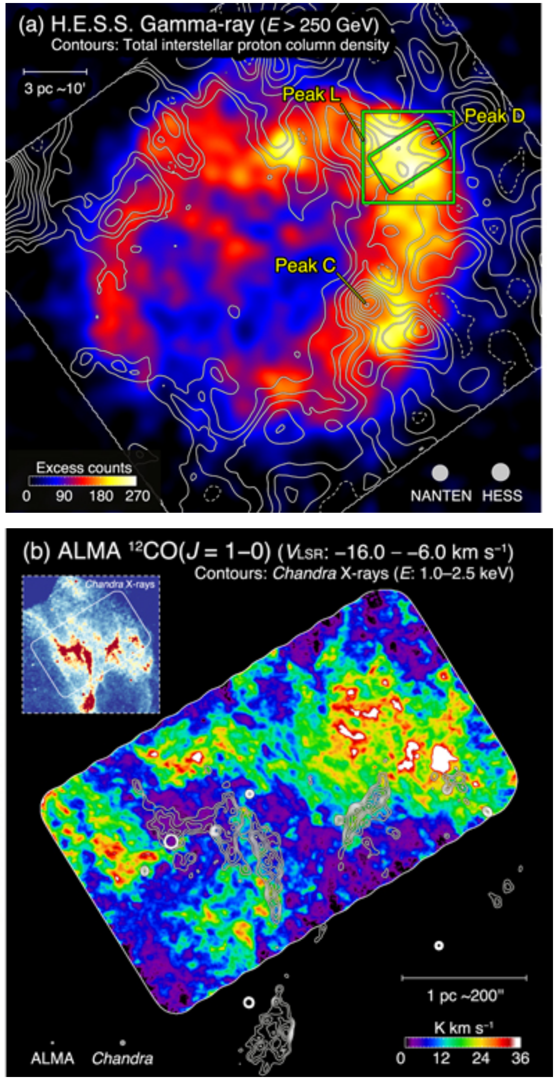

H. Sano *et al* 2020

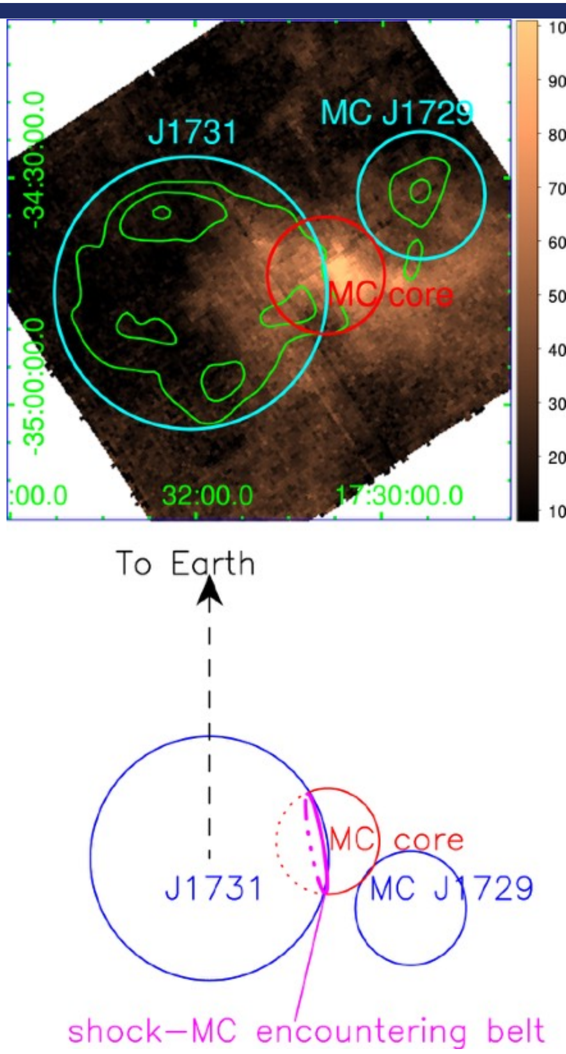

Y.Cui *et al* 2019

Stellar clusters

A nascent outflow extending from Westerlund 1

ISM gradient leading to preferential direction

Outflow could be transporting CRs out of the galactic disc

CR acceleration in stellar clusters occurring predominantly from the termination shock of a collective wind.

Resulting gamma-ray emission from the wind-blown bubble

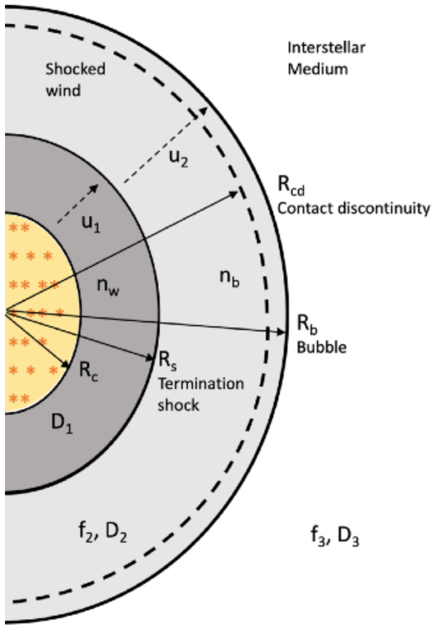

preliminary

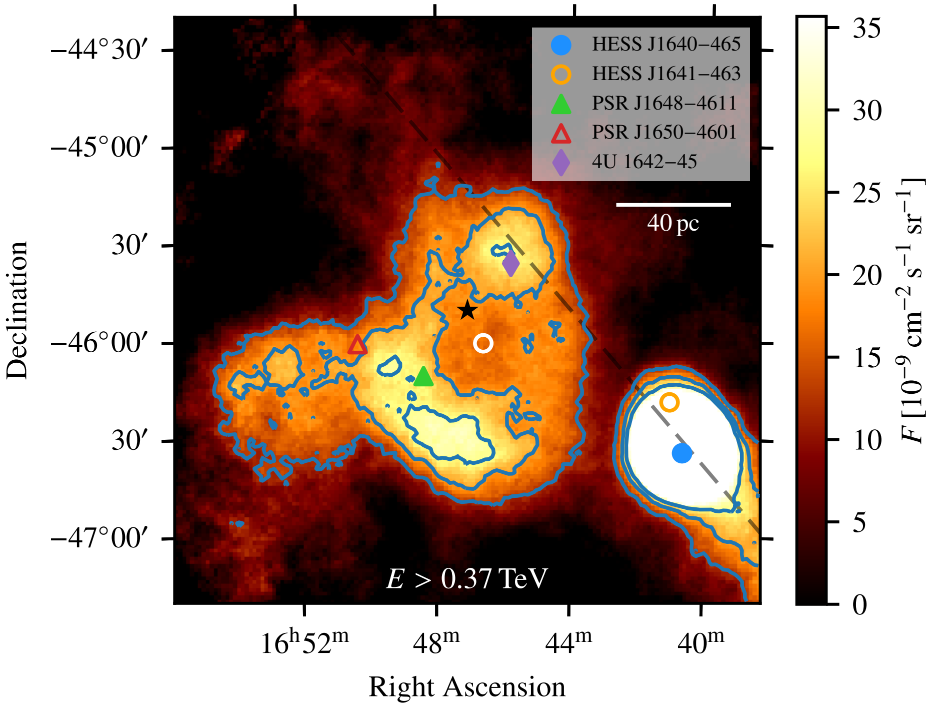

H.E.S.S. coll. 2022

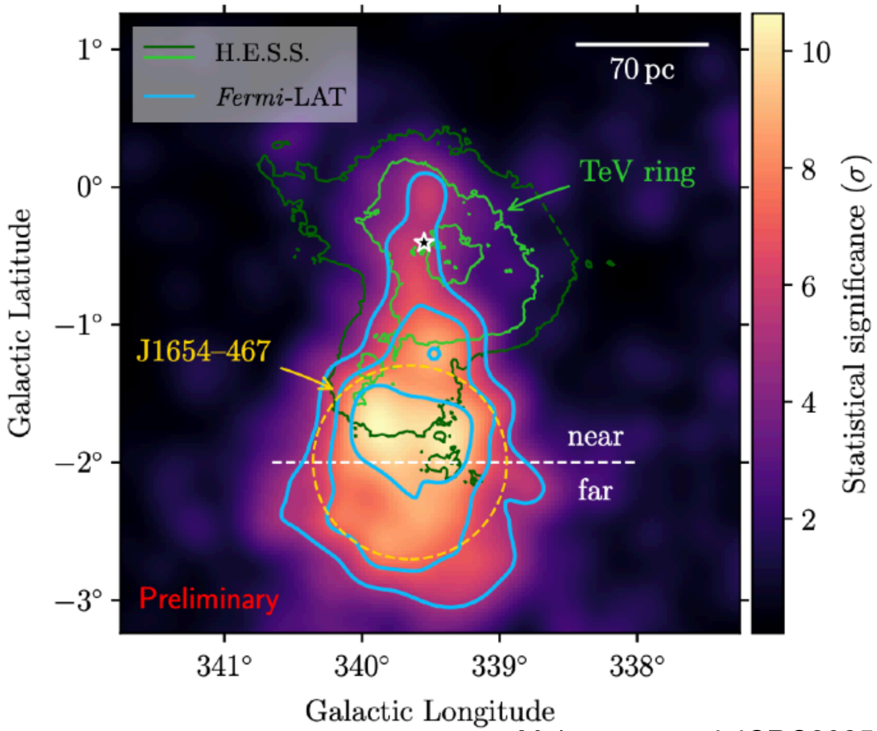

Mohrmann et al. ICRC2025

Molecular clouds in stellar cluster environments - polarisation data

Gamma-ray emission traces particle interactions
ALMA data corroborates this with evidence for cosmic ray interactions

Can use ALMA polarisation data to estimate the B-field, then estimate CR diffusion from B-field turbulence.

$$P(k) = \frac{1}{2}\mathscr{F}\left[S_2(l)\right]$$

(Strength of CR coupling to turbulence is set by turbulent power at the corresponding gyro-scale)

$$D \propto \frac{1}{P(k)}$$

Example: HESS J1848-018 (W43) potentially emission from a massive star cluster

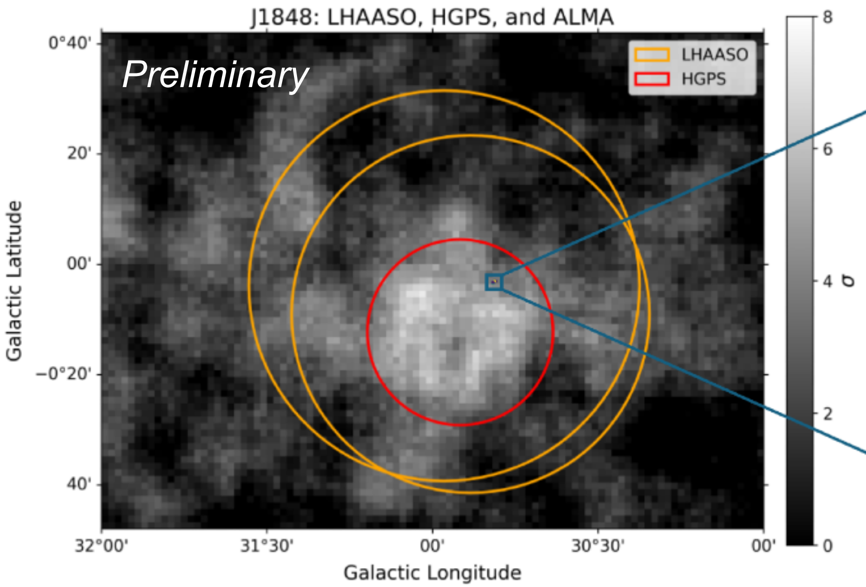

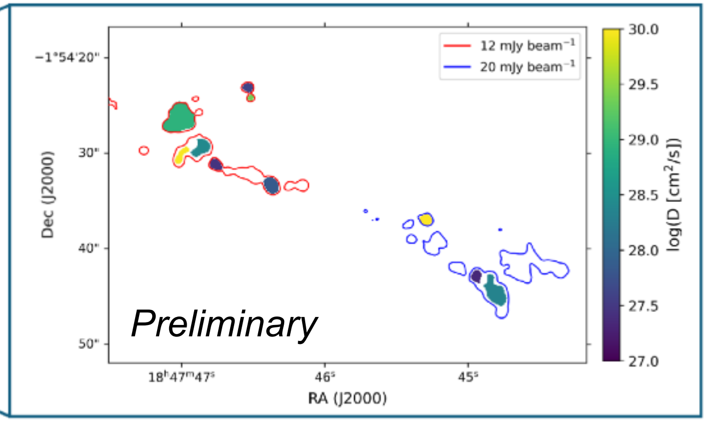

S.-T. Chen, E. Owen

Characterising CR diffusion within a cloud empirically

Sub-mm dust polarisation —> magnetic field structure

Power spectrum of turbulence can be used to obtain a diffusion coefficient

Owen et al. 2021

Pulsar Wind Nebulae

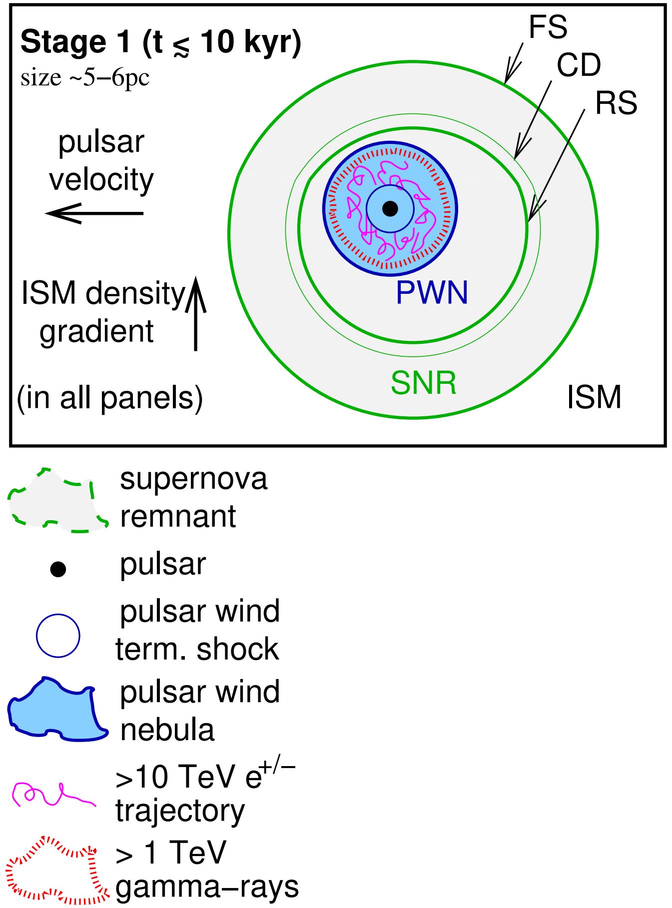

Giacinti, AM, Lopez-Coto et al 2020

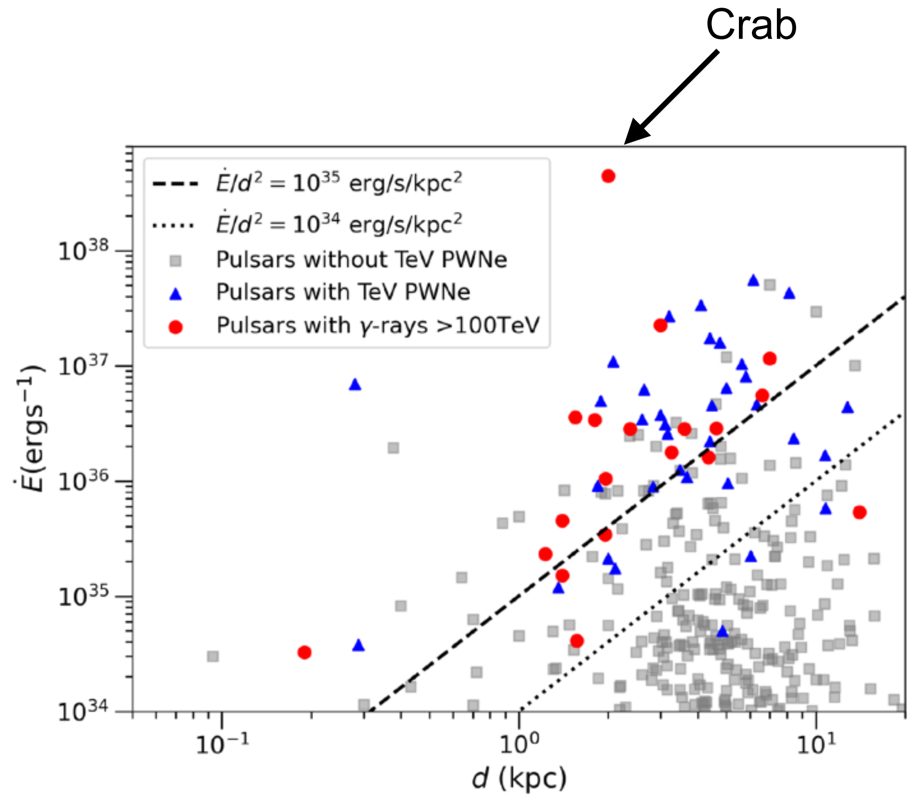

AM & Gelfand 2022

Crab pulsar wind nebula —> up to PeV

A sub-dominant hadronic component could be revealed at the highest energies, beyond the Klein-Nishina cut-off

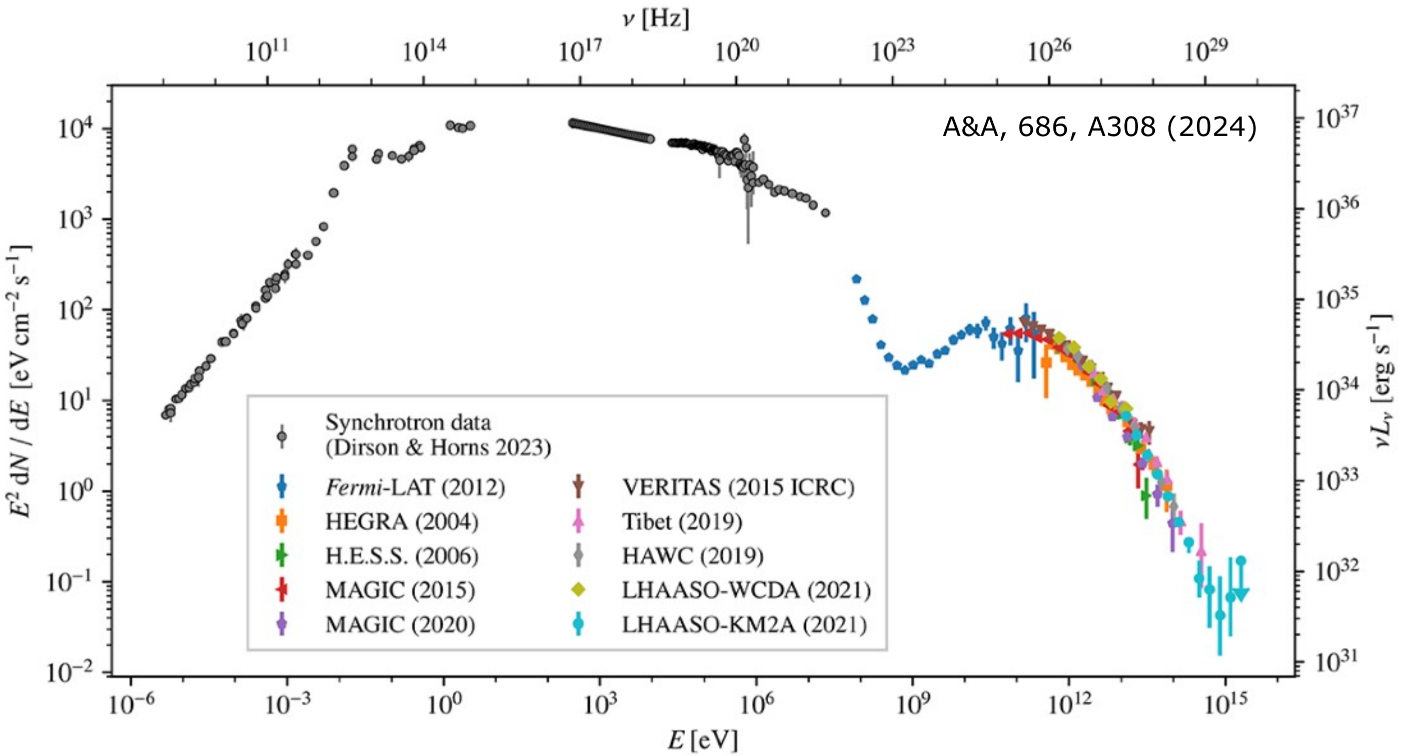

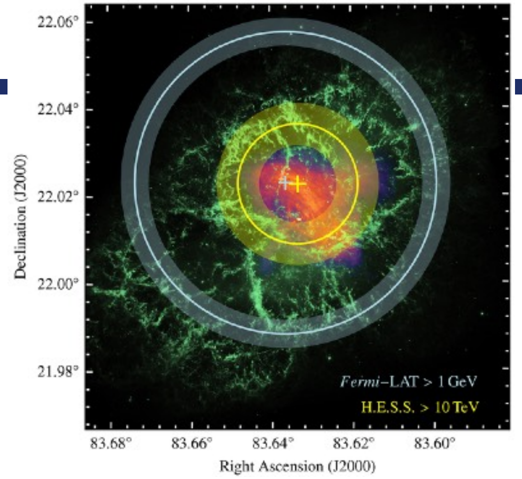

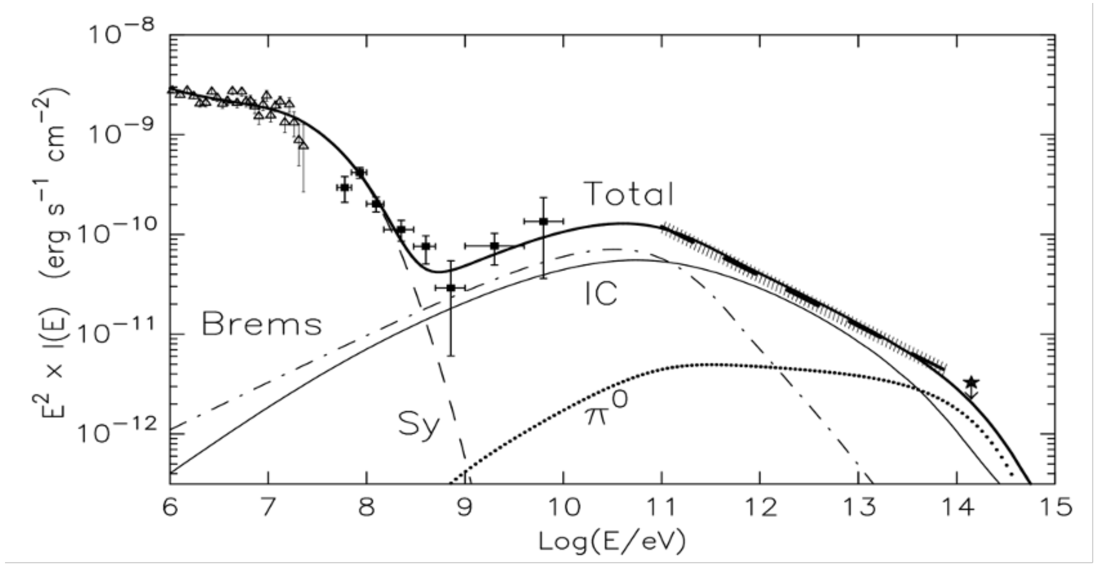

Aharonian & Atoyan (1998)

How could hadrons reach high energies in the environment of the Crab PWN?

See also Nie et al. 2022

Acceleration of hadrons in PWNe

Model: Re-injection of particles from the reservoir within the supernova remnant

Further hadronic particle acceleration at the pulsar wind termination shock

Particle tracking simulations:

Assume Bohm diffusion inwards and outward advection with the wind
Particles undergo a factor 2 energy gain per shock crossing

(Spencer et al 2025)

Assume a power law spectrum of particles injected into the PWN from the SNR reservoir with energies between 1 and 50 TeV

(See also Ohira et al 2018;
Lucek & Bell 1994)

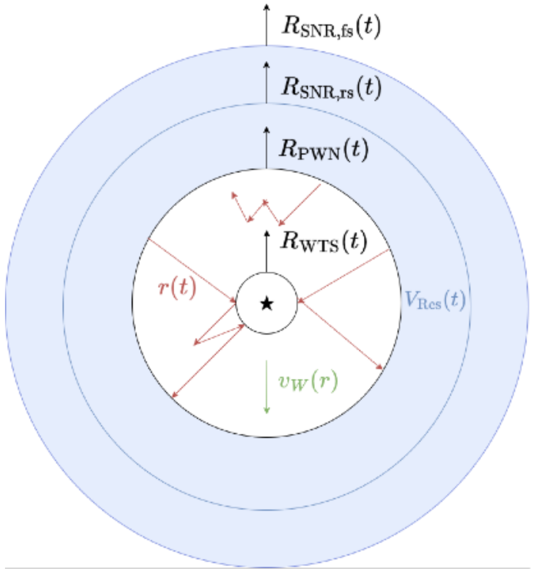

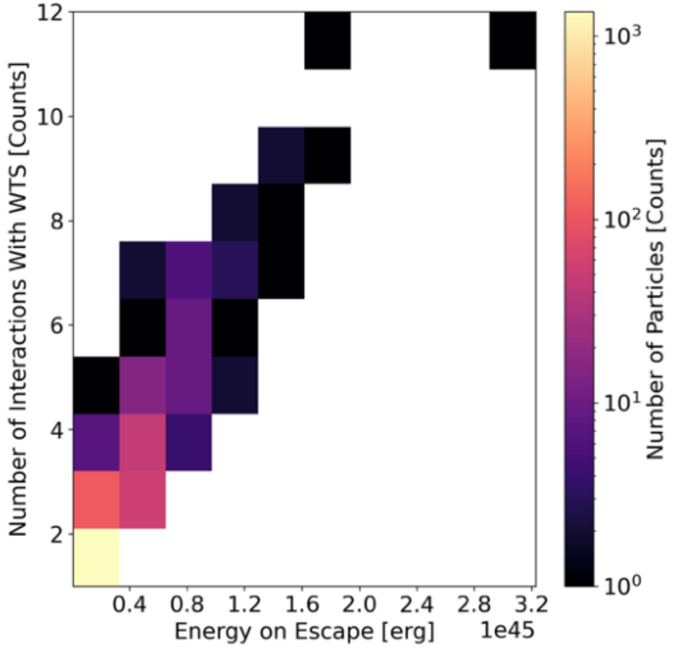

Acceleration of hadrons in PWNe

Resulting spectrum of re-accelerated particles escaping from the Crab PWN at the current time can match to LHAASO data at ~1 PeV.

(Spencer et al 2025)

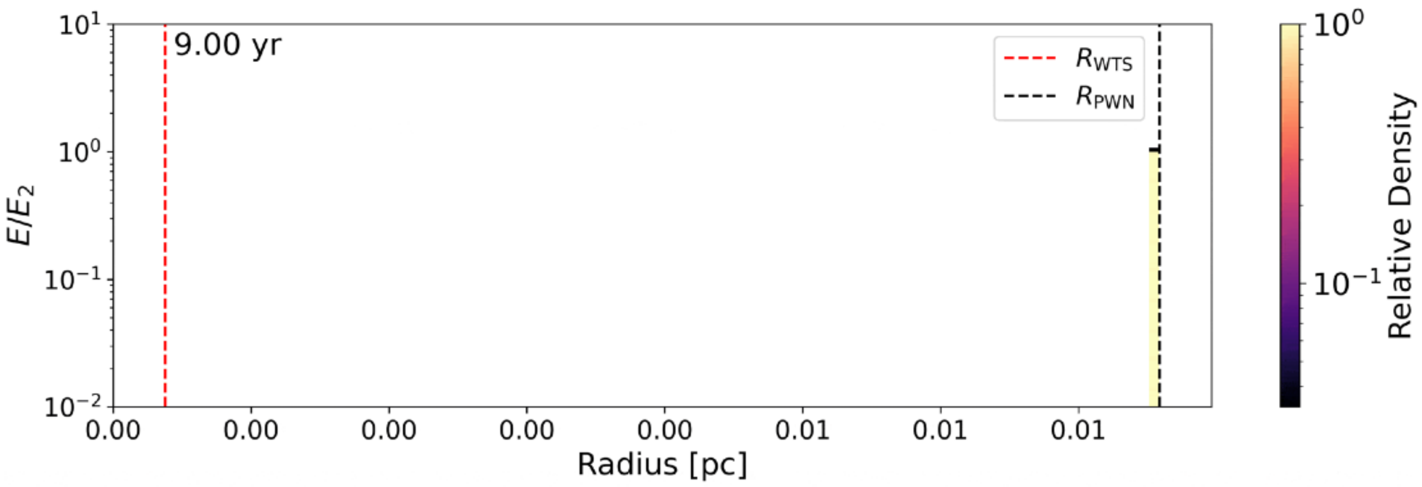

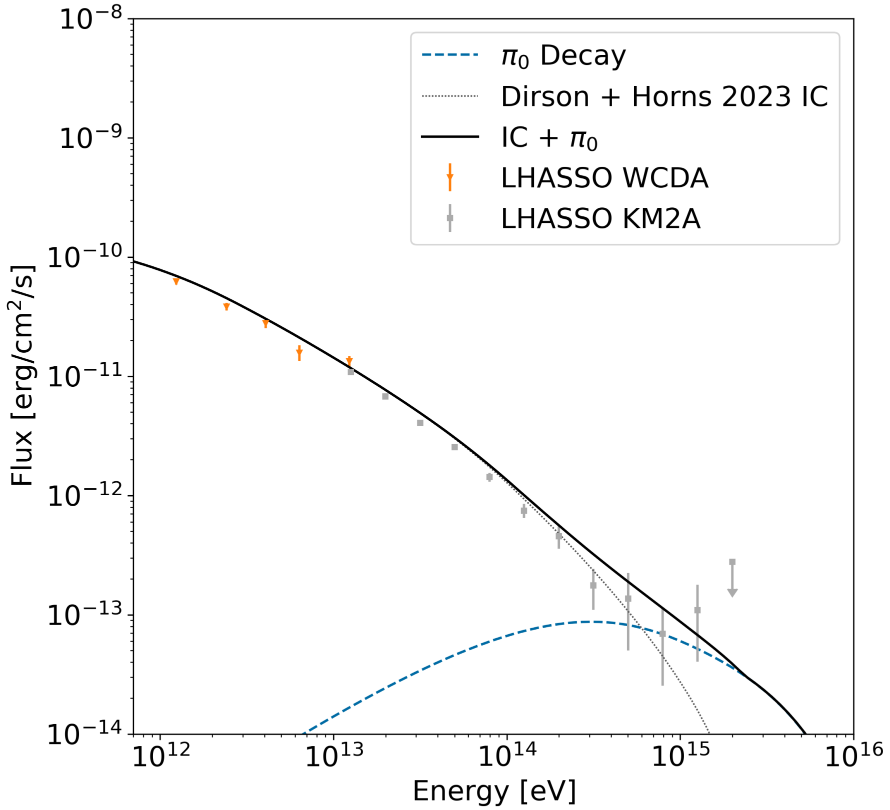

Nuclei from the pulsar surface reaching the wind?

Cascade multiplicity

Extraction of nuclei from pulsar surface and ion acceleration; mixed composition enters pulsar wind. e.g. Kotera et al., JCAP 08, 26 (2015)

Ions can carry up to 20% of energy, acceleration at termination shock,
e.g. Lemoine et al. 2015

Max ion energy and injection depends on pair-production multiplicity

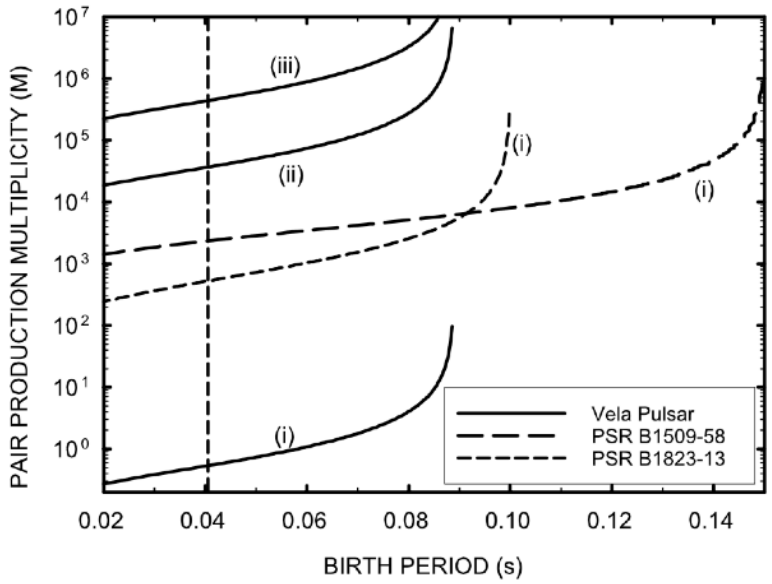

de Jager 2007

Constraining the pair-production multiplicity (κ) constrains the fraction of energy carried by ions in the wind.
Lower kappa — better for ions.

$$\langle \kappa \rangle = \frac{N_{\rm el}}{2N_{\rm GJ}}$$, where the Goldreich-Julian number:

$$N_{\rm GJ} = \int_{t=0}^{t=-\tau(P_0)} \frac{[6c\dot{E}(t)]^{1/2}}{e}(-dt)$$

With the number of electrons $N_{\rm el}$ from modelling gamma-ray spectra, we can obtain curves of $\langle \kappa \rangle$ as a function of P_0

Nuclei from the pulsar surface reaching the wind?

Where the "true" size of the PWN and SNR are known (e.g. from radio observations) we can approximately obtain P_0 :

$$P_0 = 2\pi \left[\frac{2E_0}{\eta_1 I} \left(\frac{R_{PWN}}{\eta_3 R_{SNR}} \right)^3 + \left(\frac{2\pi}{P_t} \right)^2 \right]^{-1/2}$$

van der Swaluw & Wu (2001)

The intersection of the estimates for P_0 and curves for κ provide a constrained estimate for κ .

For hadrons to reach the wind, κ must be below a value $\langle\kappa\rangle_{\rm lim}$ that we obtain for 3 PeV hadrons under the assumption of an efficiency factor $0.1 \leq \eta \leq 1$

de Oña Wilhelmi et al 2022

Shown for 6 pulsars using H.E.S.S. and MWL data

—> hadron escape can be ruled out for PSR J1747-2809 only

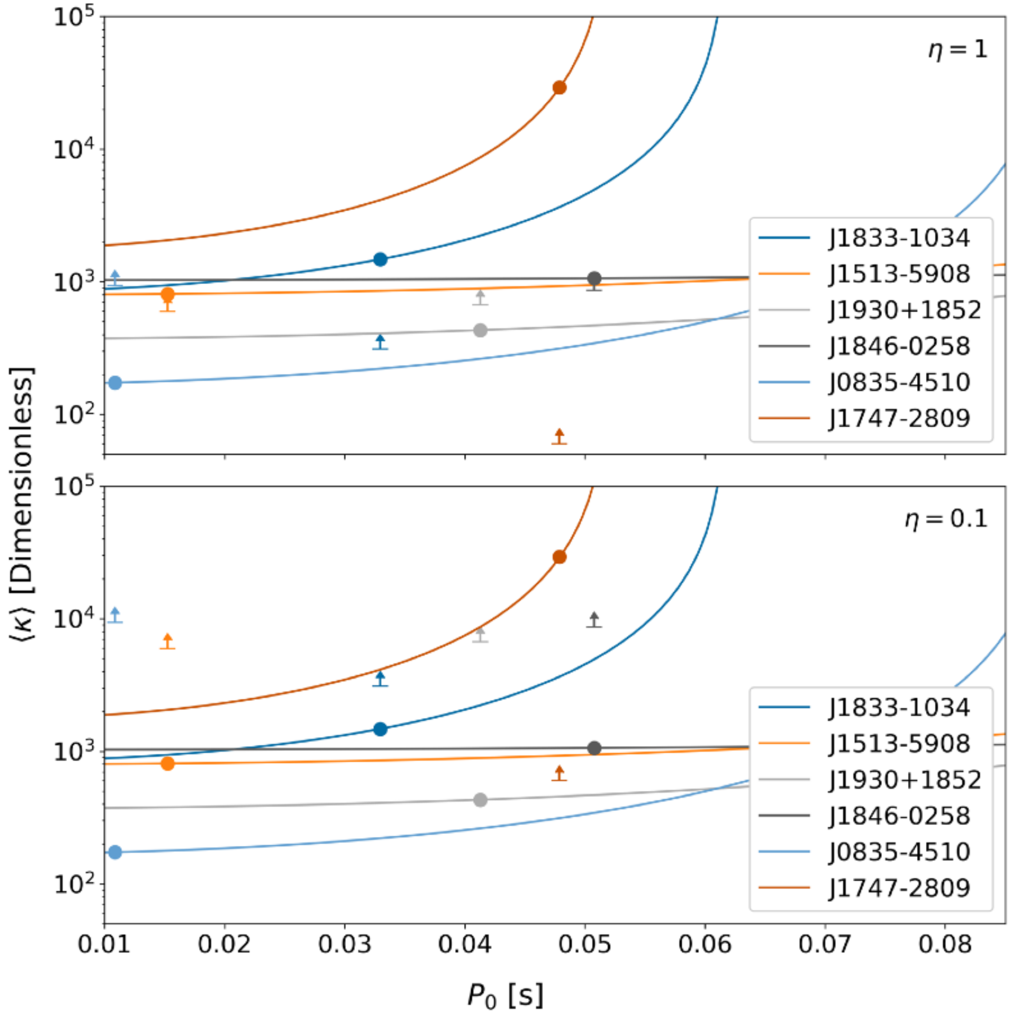

Spencer & AM 2025

Pulsar Wind Nebulae

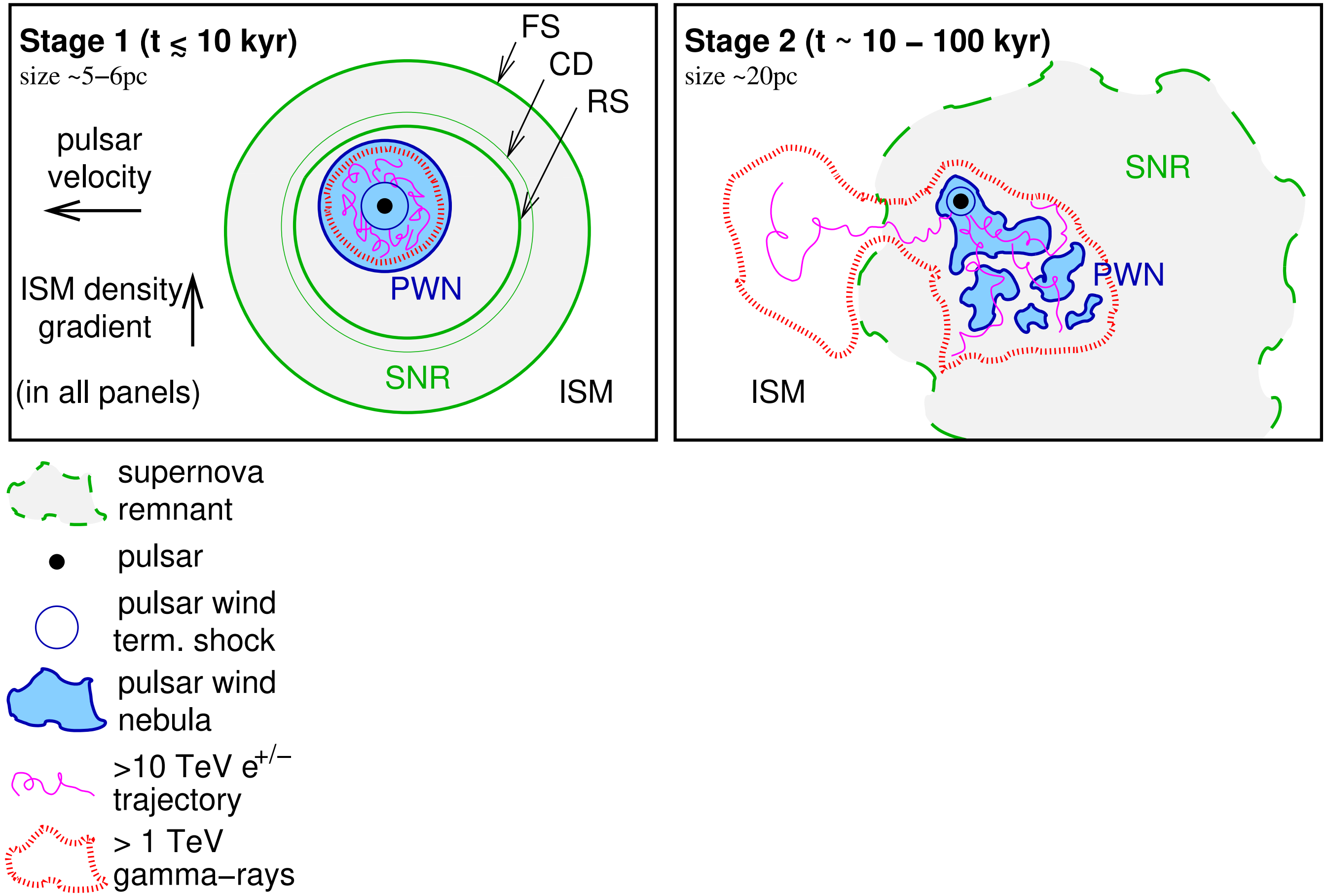

Giacinti, AM, Lopez-Coto et al, 2020

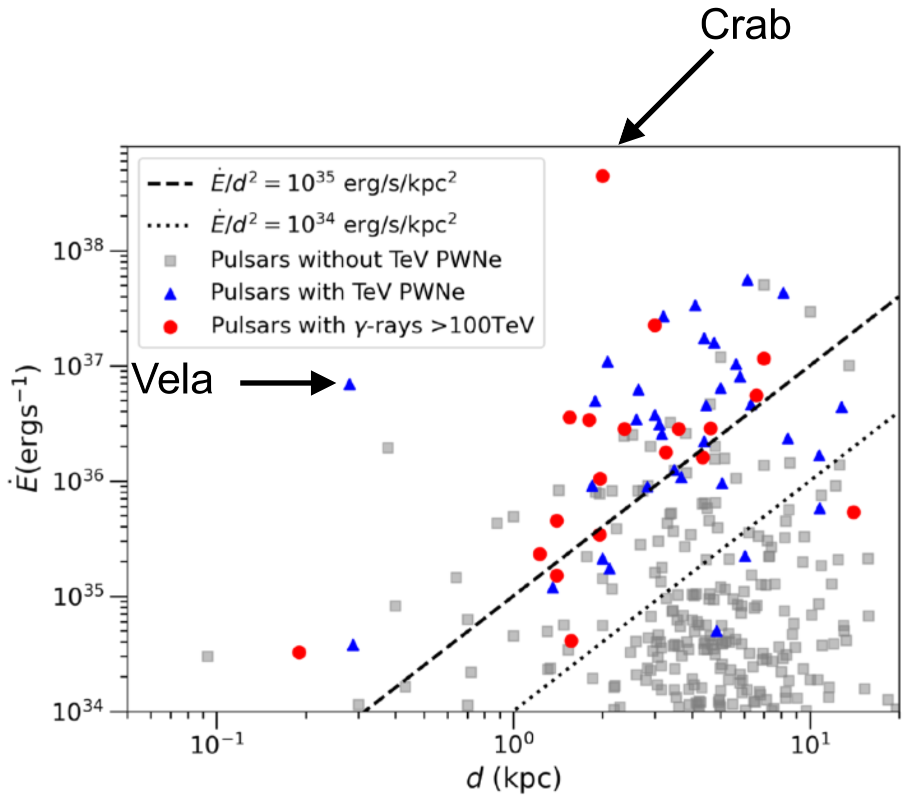

AM & Gelfand (2022)

Pulsar Wind Nebulae: Vela X

Vela pulsar (PSR B0833-45)
$\tau_c = 11.3$ kyr ;
$\dot{E} = 6.9 \times 10^{36}$erg/s
Distance: 290 pc

— may account for high energy cosmic ray electrons

X-ray + gamma-ray: Synchrotron and inverse Compton emission from same electron population

Map the magnetic field strength across the region (5 - 12 μG)
Near constant within cocoon, strong to north

1-5 keV eROSITA
(Mayer et al 2023)

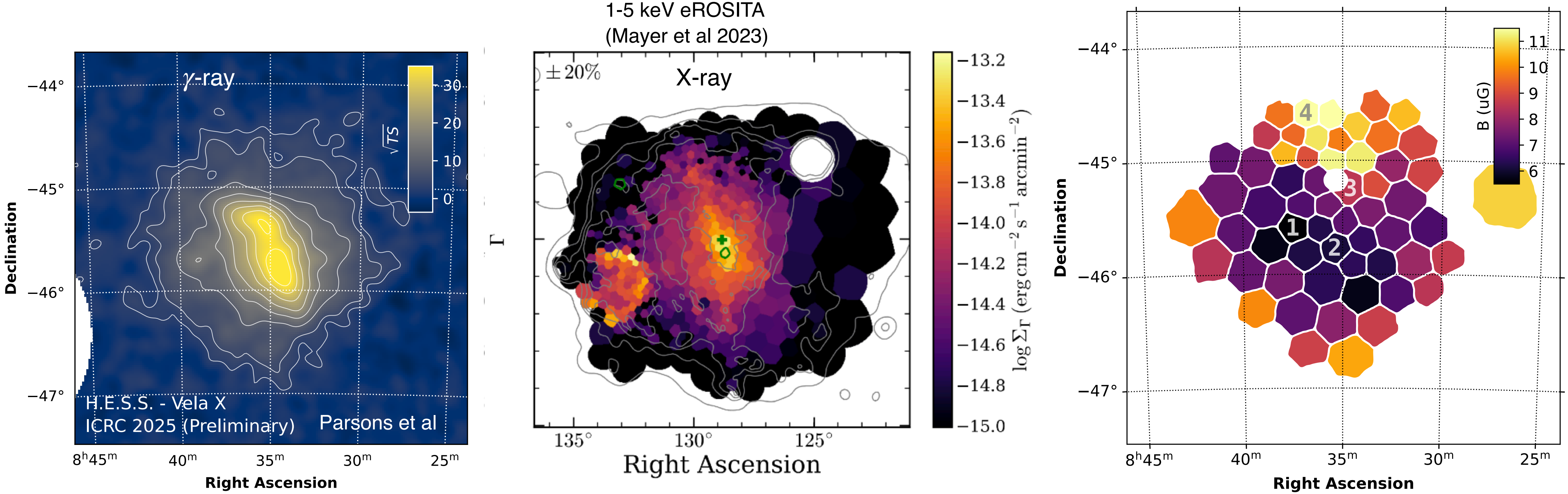

Energy-dependent morphology in PWNe

PSR B1823-13
$\dot{E} = 2.8 \times 10^{36}$erg/s
$\tau_c = 21.4$ kyr
Distance: 3.9 kpc

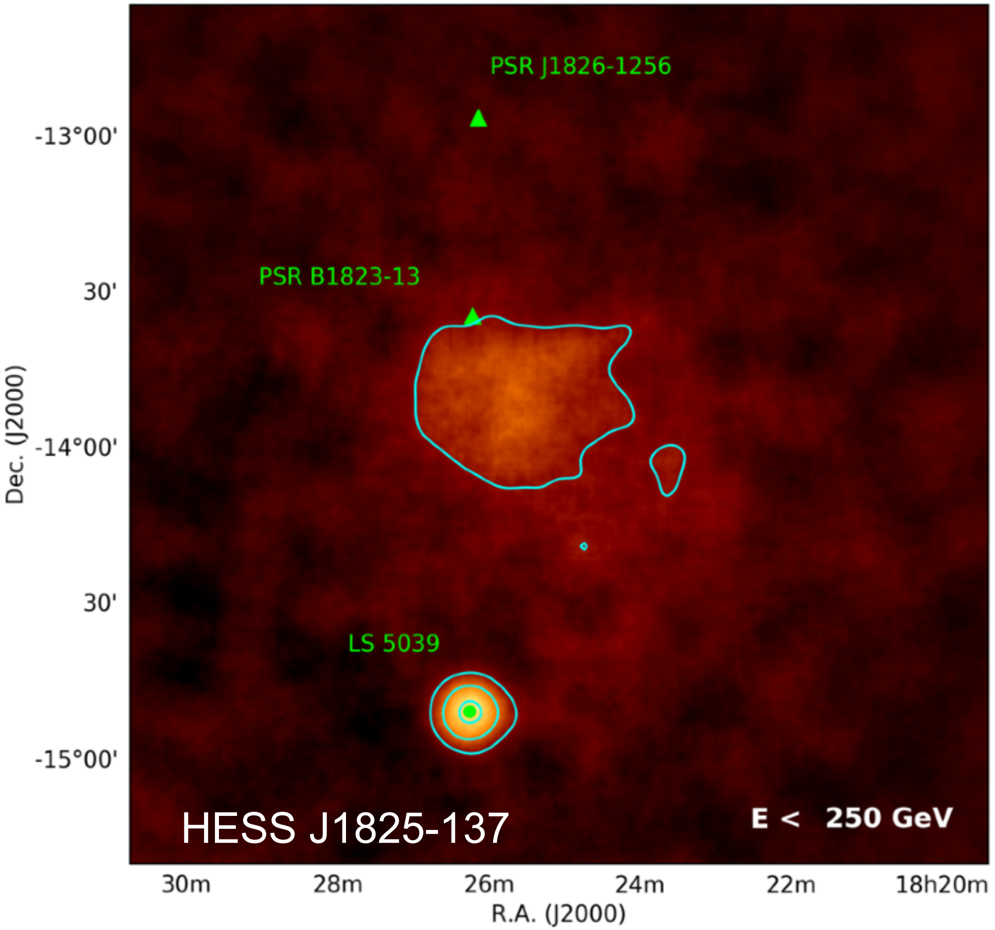

Electrons lose energy with distance from the pulsar

$R \propto E^{\alpha}$, where α can be related to diffusion δ and advection β

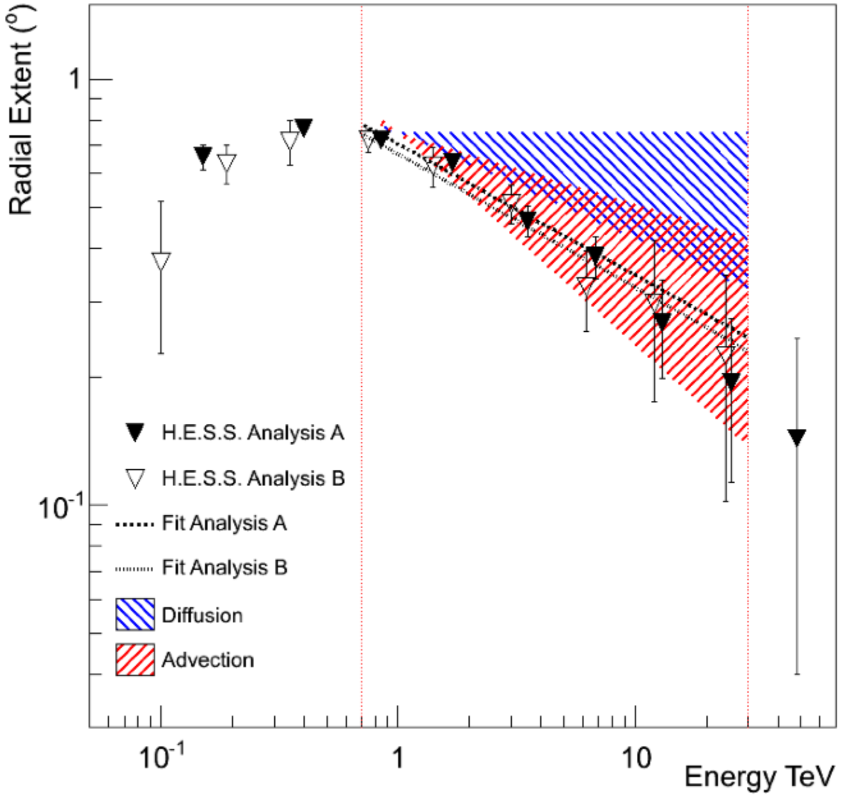

H.E.S.S. coll. (2019)

Energy-dependent morphology in PWNe

Energy-dependent morphology as a common feature of pulsar environments
→ electron transport and cooling
→ leptonically dominant sources

spectral index increasing with distance from pulsar

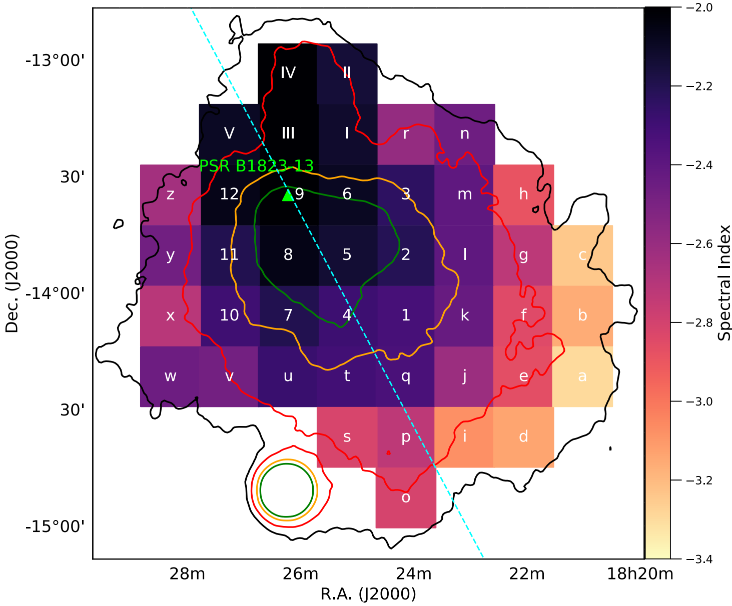

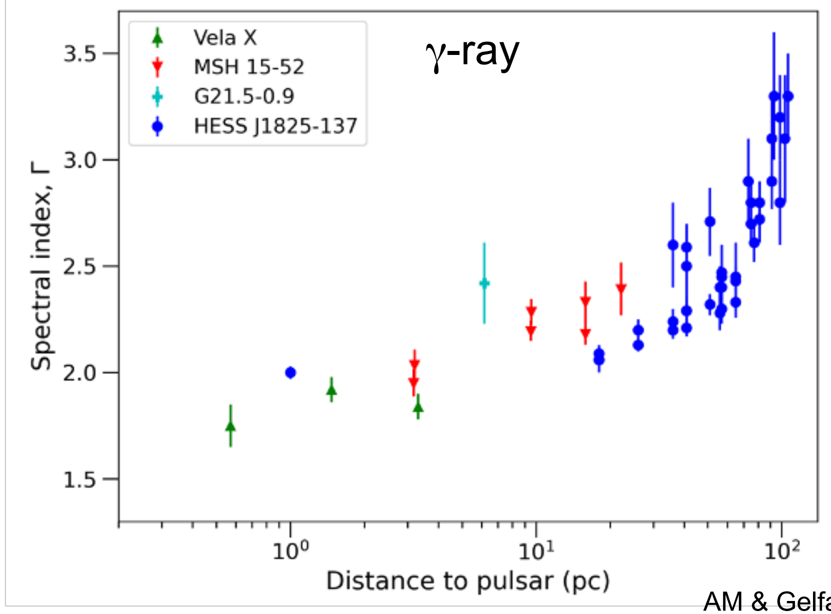

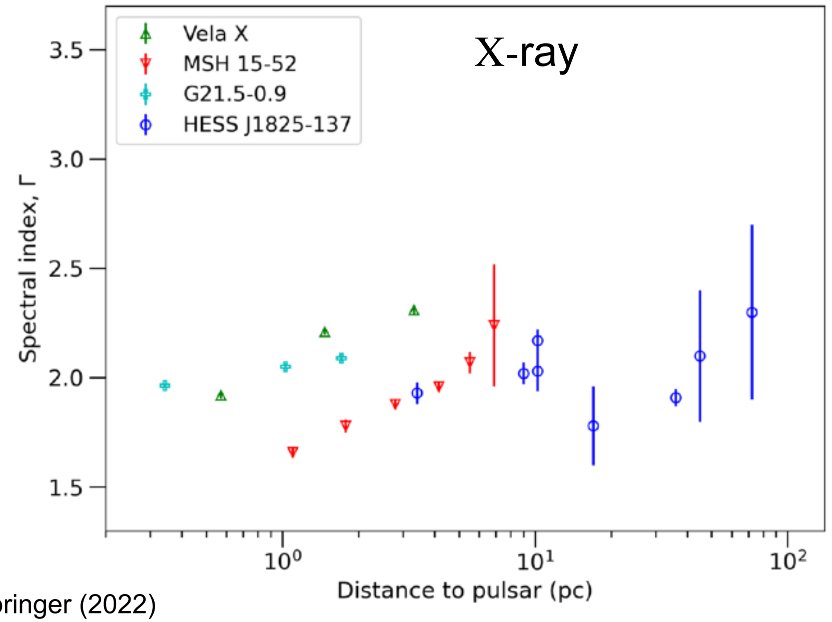

AM & Gelfand, Springer (2022)

Pulsar Wind Nebulae

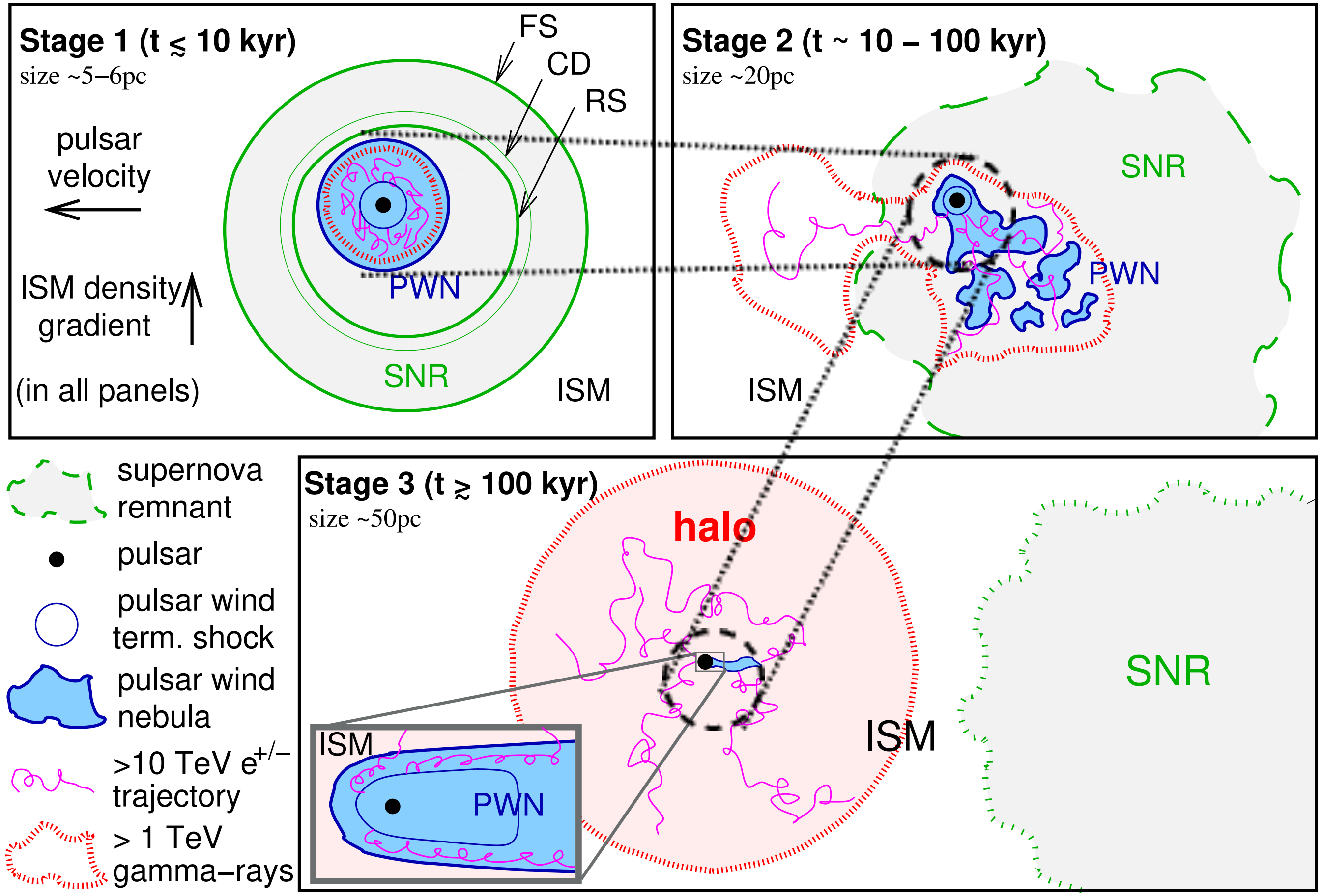

Giacinti, AM, Lopez-Coto et al, (2020)

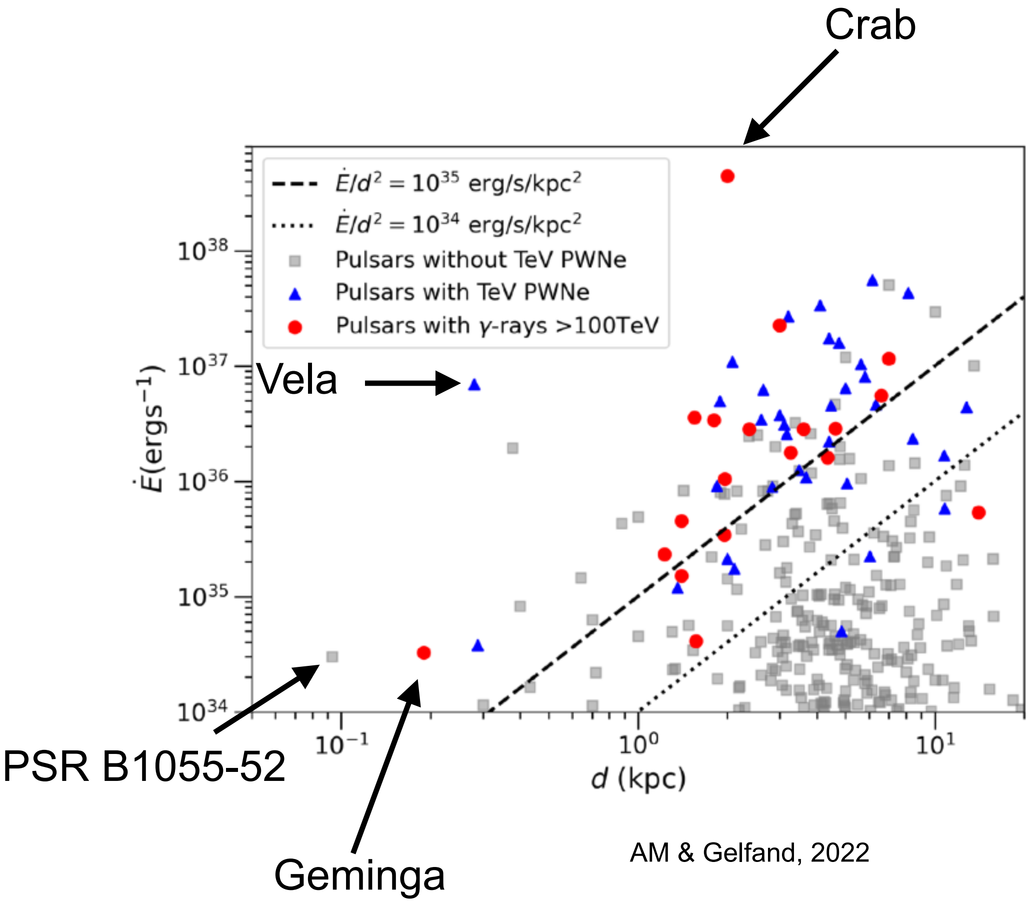

AM & Gelfand, 2022

Diffusion modelling of the Geminga pulsar halo

$\tau_c = 342$ kyr ; $\dot{E} = 3.2 \times 10^{34}$erg/s ; Distance: 140-250 pc

Gamma-ray emission >> X-ray size
Model of continuous electron injection by the pulsar and diffusion through the halo

Diffusion Coefficient normalisations significantly below galactic average preferred
Consistent with findings by other gamma-ray facilities

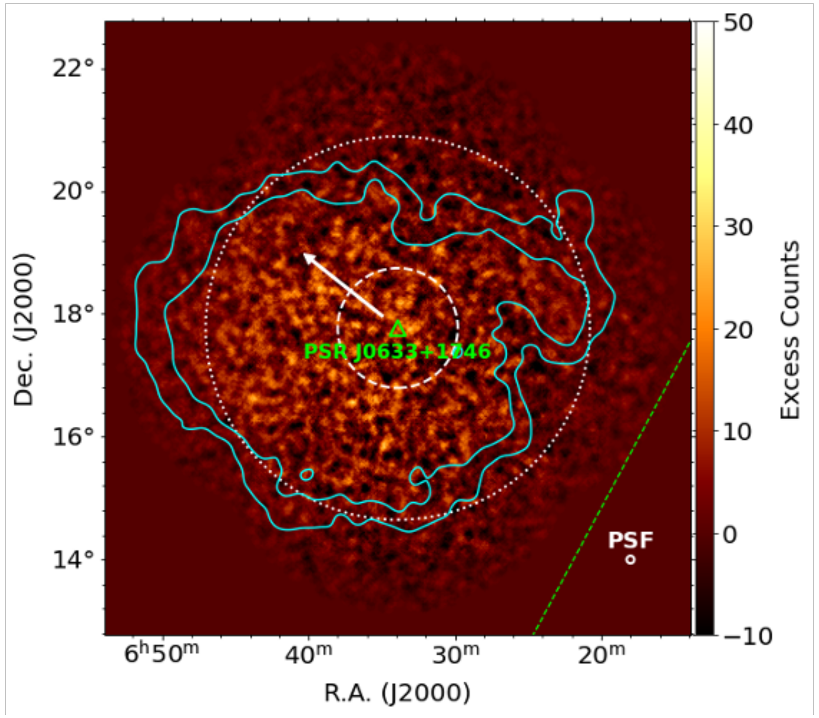

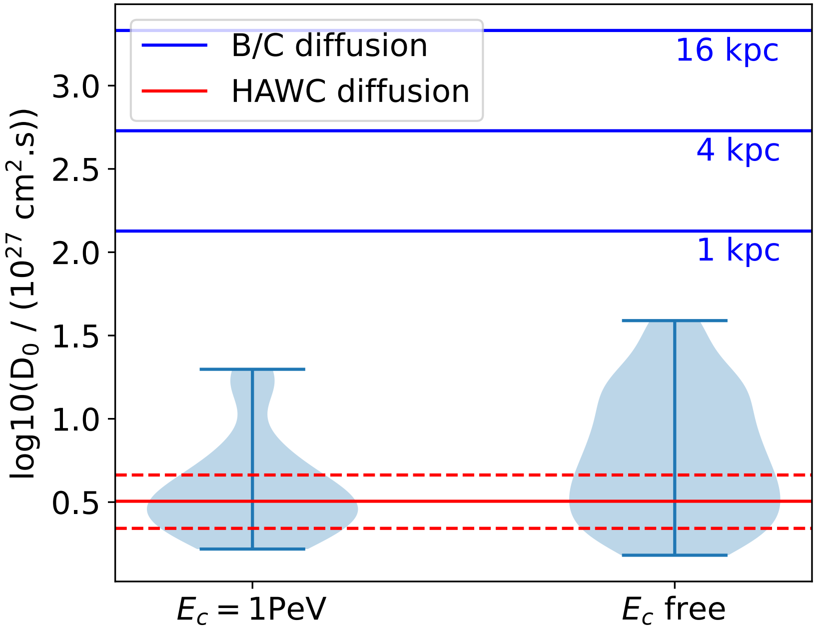

H.E.S.S. coll. (2023)

PSR B1055-52 — a newly discovered pulsar halo

Age $\tau_c = 535$ kyr ;
Spin-down power $\dot{E} = 3.0 \times 10^{34}$erg/s

Distance: 90 pc — 750 pc , at l = 285.98°, b = 6.65°

Source significance $15.9\ \sigma$

Best fit model:
2D Gaussian spatial model ($\sigma \approx 2^{\circ}$)
and power law spectral model

Diffusion modelling — suppressed with respect to ISM values, consistent with other halos

First halo discovered by IACTs, located in southern hemisphere, potentially the oldest and closest so far.

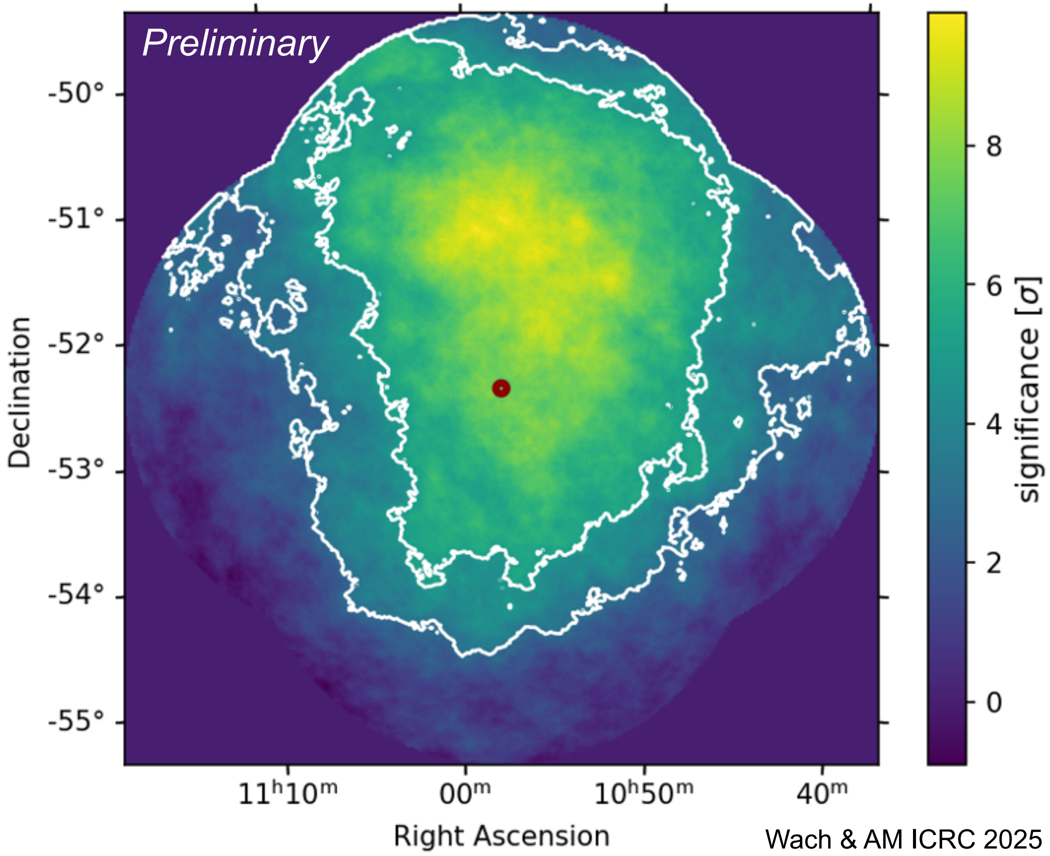

Wach & AM ICRC 2025

Cosmic Ray Electron Spectrum and Pulsars

Recent measurements of slow diffusion in vicinity of nearby accelerator

Generally need a local source contribution to explain the high energy CR electron spectrum

Either the diffusion coefficient recovers to galactic values, or there is another local source contributing

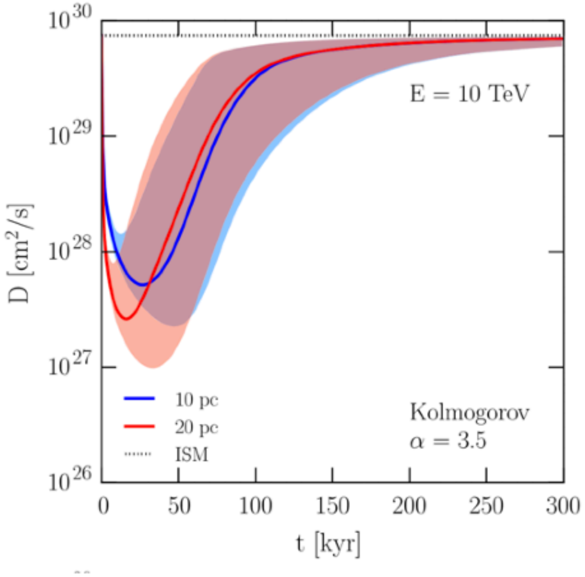

Evoli et al 2018

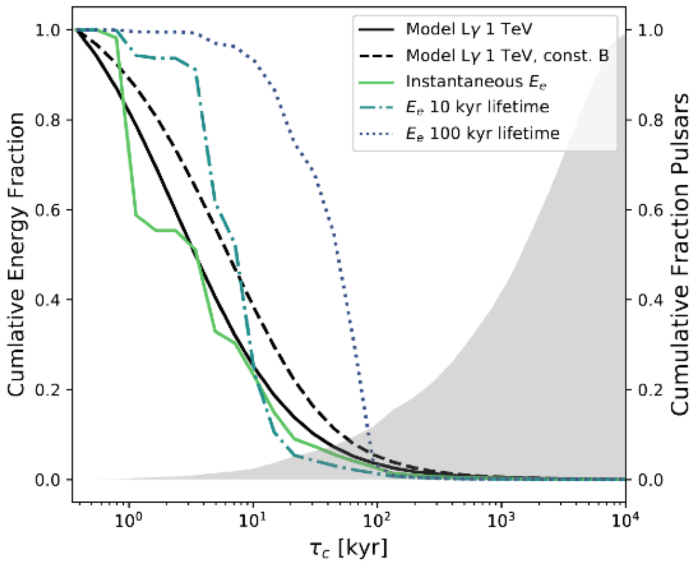

Giacinti et al 2020

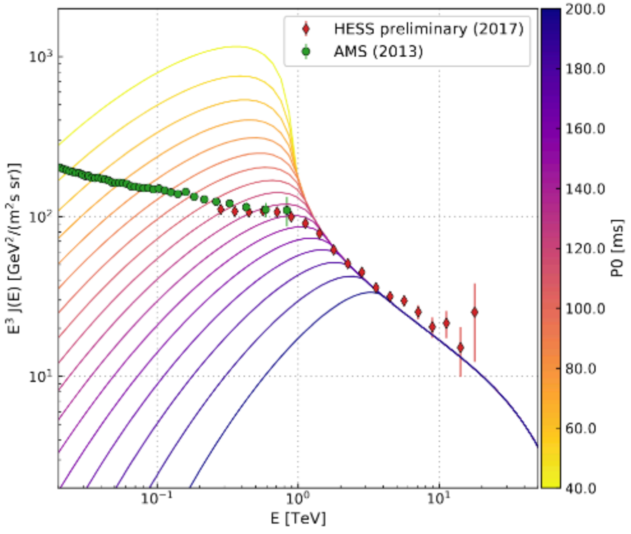

Lopez-Coto et al. 2018

Summary & Outlook

Several source classes are capable of accelerating CRs to energies $\gtrsim 10^{15}$ eV (SNRs, PWNe, stellar clusters, μQSRs…)

However, the most energetic particles can escape the source at early times
(non-continuous acceleration)

Therefore, at the highest energies, we may anticipate an increasing fraction of **passive** UHE sources,
such as clouds illuminated by CRs from nearby active accelerators

This can be used to search for evidence of past PeVatron activity.

CR transport can be probed via MWL emission using a variety of approaches (gamma-ray morphology, radio polarisation…)

Reconciling the different length scales on which these techniques are applicable can help yield a more coherent picture of CR transport within complex environments.

Evidence in multiple sources for particle leakage into the medium surrounding an accelerator

Friedrich-Alexander-Universität
Erlangen-Nürnberg

Erlangen Centre for Astroparticle Physics

Thank you for your attention
Any questions?

alison.mw.mitchell@fau.de

Very-High-Energy Gamma-ray Sky

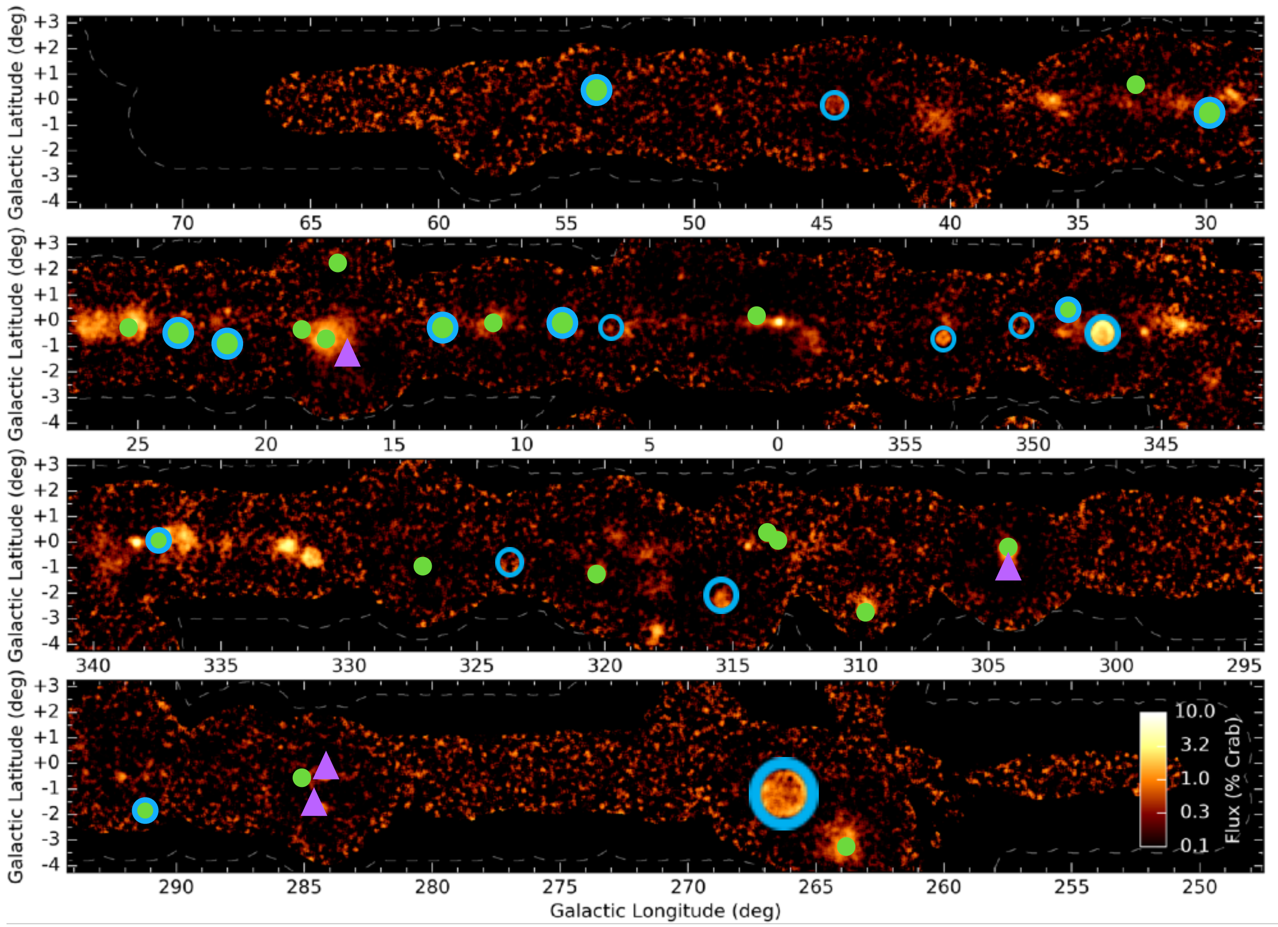

H.E.S.S. A&A **612** A1 (2018)

H.E.S.S. Galactic plane survey : 78 sources

2700 hours of observations from 2004-2013

LHAASO (particle detector array) in 2024 :
43 “ultra-high-energy” sources > 100 TeV
Highest energy photons ever ~2.5 PeV from Cygnus region

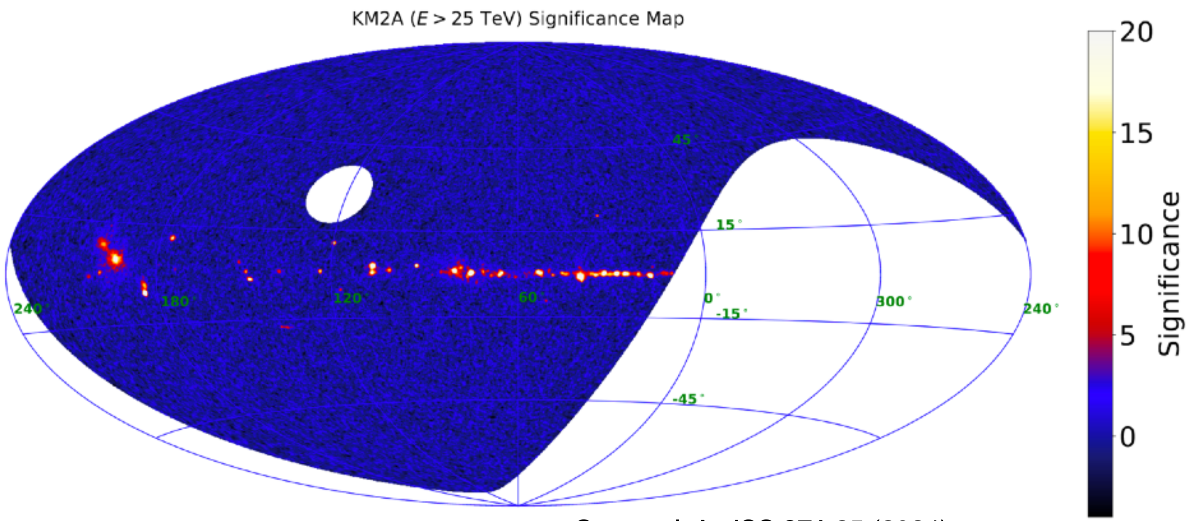

Cao et al. ApJSS **271** 25 (2024)

Pulsar Wind Nebulae

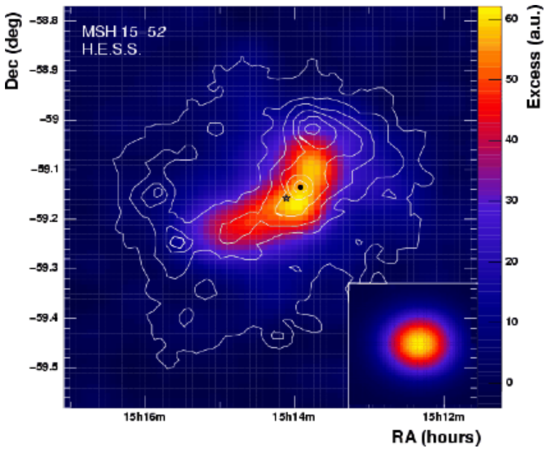

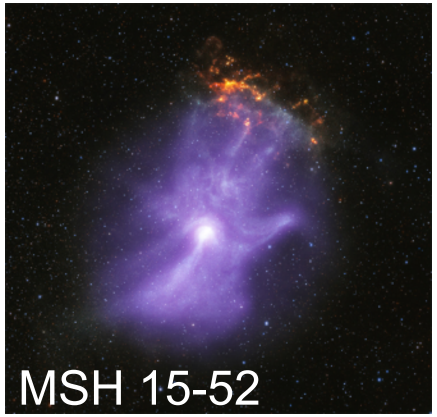

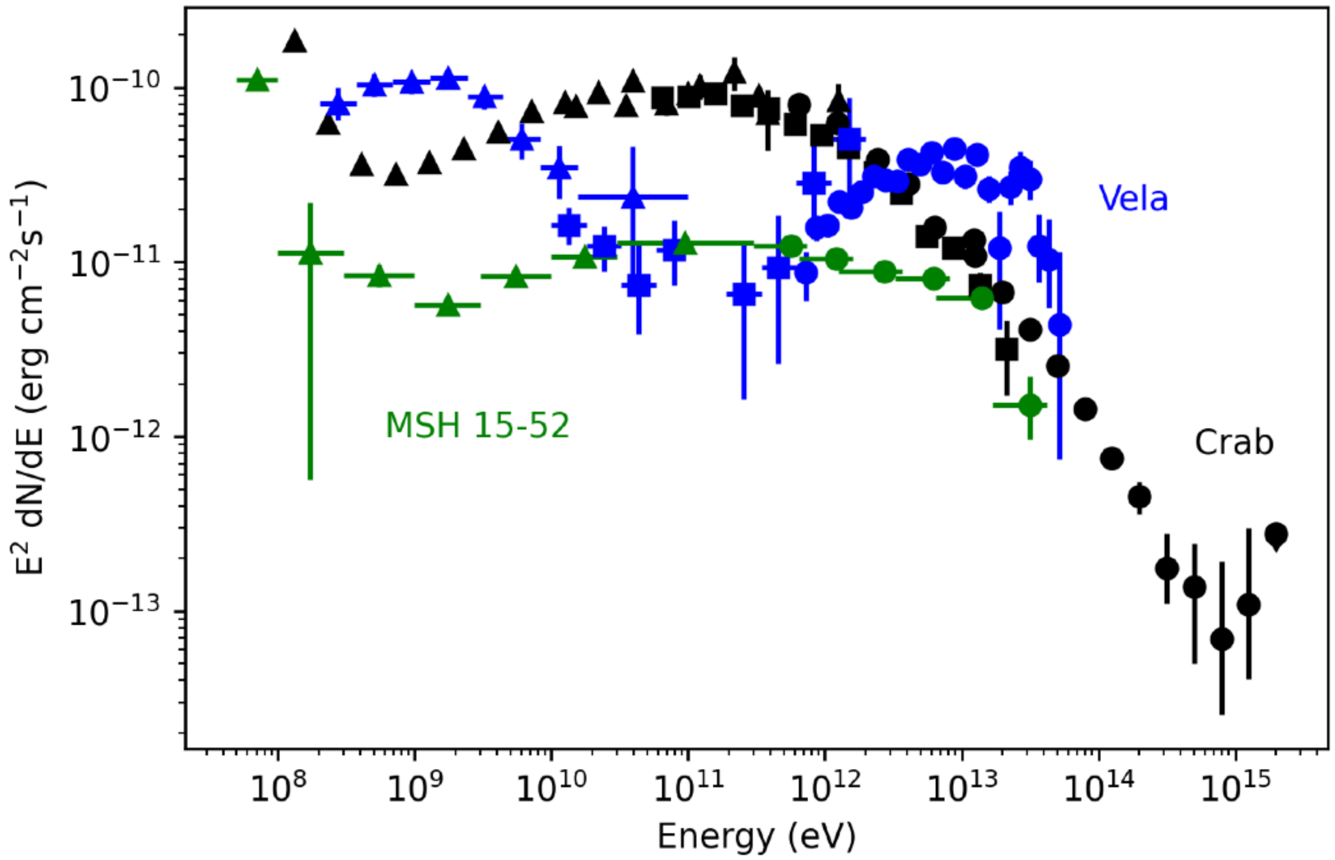

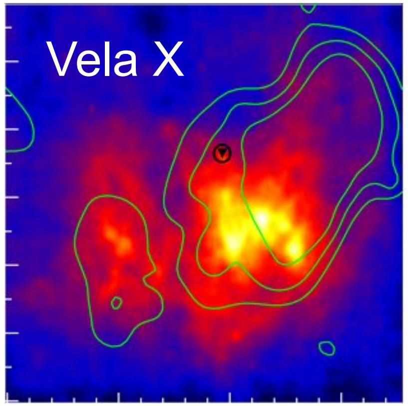

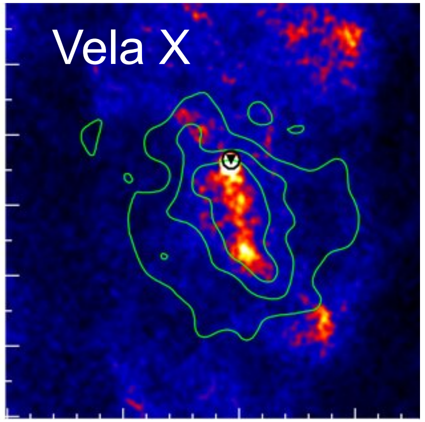

AM & Gelfand, Springer (2022)

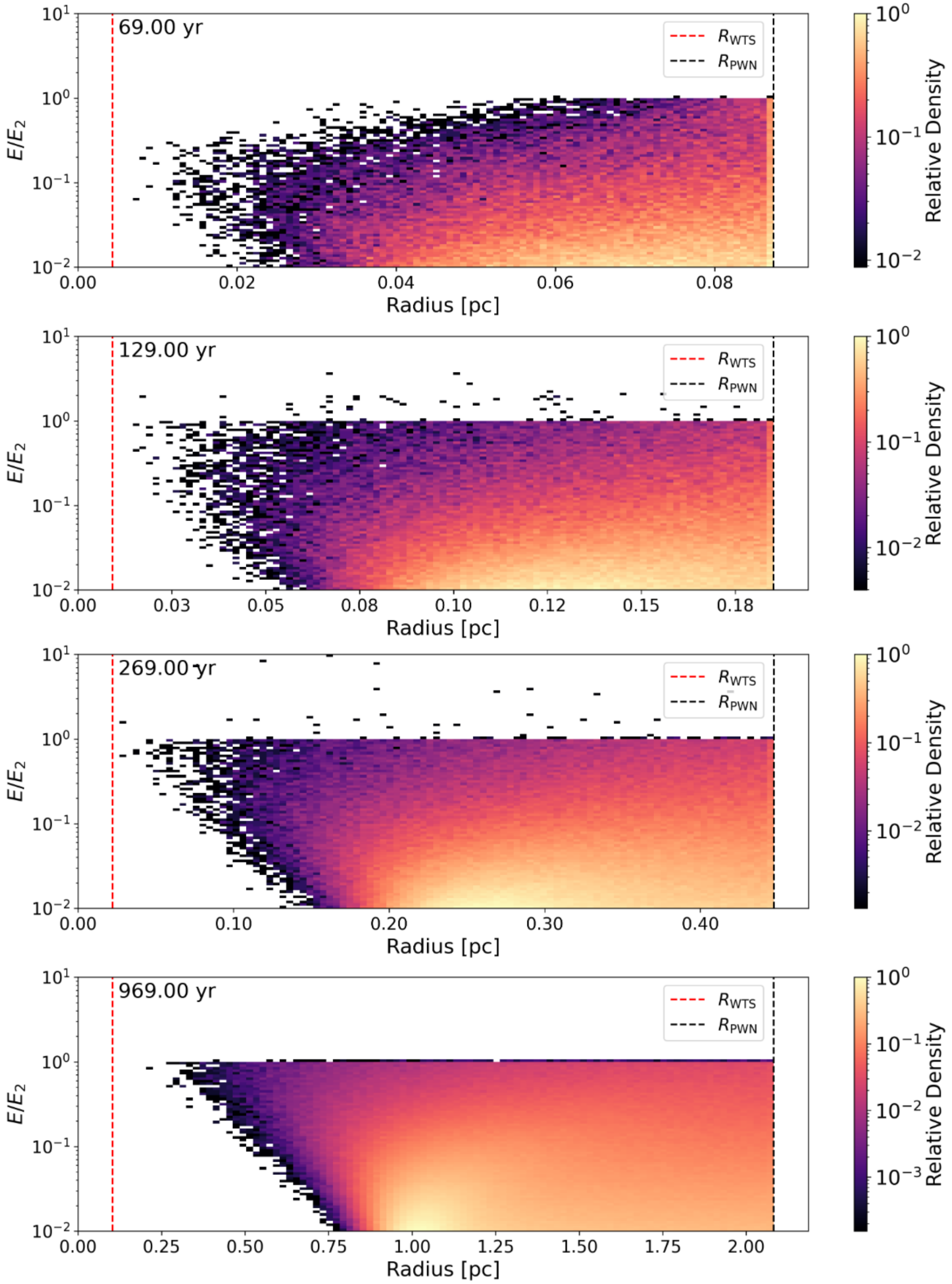
69.00 yr
129.00 yr
269.00 yr
969.00 yr
R_{WTS}
R_{PWN}
E/E_2
Radius [pc]
Relative Density
10^{1}
10^{0}
10^{-1}
10^{-2}
10^{-3}
0.00
0.02
0.04
0.06
0.08
0.03
0.05
0.10
0.12
0.15
0.18
0.20
0.30
0.40
0.25
0.50
0.75
1.00
1.25
1.50
1.75
2.00